Dr Carlson

X-651-72-178
PREPRINT

THE DEVELOPMENT OF HURRICANE INEZ, 1966, AS SHOWN BY SATELLITE NIGHTTIME RADIOMETRIC AND DAYTIME TELEVISION COVERAGE

LEWIS J. ALLISON

MAY 1972

GSFC
GODDARD SPACE FLIGHT CENTER
GREENBELT, MARYLAND

X-651-72-178
PREPRINT

THE DEVELOPMENT OF HURRICANE INEZ, 1966, AS SHOWN BY SATELLITE NIGHTTIME RADIOMETRIC AND DAYTIME TELEVISION COVERAGE

by

Lewis J. Allison
Laboratory for Meteorology and Earth Sciences

May 1972

GODDARD SPACE FLIGHT CENTER
Greenbelt, Maryland

THE DEVELOPMENT OF HURRICANE INEZ, 1966, AS SHOWN BY SATELLITE NIGHTTIME RADIOMETRIC AND DAYTIME TELEVISION COVERAGE

Lewis J. Allison
Laboratory for Meteorology and Earth Sciences
Goddard Space Flight Center
Greenbelt, Maryland 20771

ABSTRACT

A complete documentation of Nimbus 2 High Resolution Infrared Radiometer data and ESSA-1 and 3 television photographs is presented for the life-time of Hurricane Inez, 1966. Ten computer produced radiation charts were analyzed in order to delineate the three dimensional cloud structure during the formative, mature and dissipating stages of this tropical cyclone. Time sections were drawn throughout the storm's life cycle to relate the warm core development and upper level outflow of the storm with their respective cloud canopies, as shown by the radiation data. Aerial reconnaissance weather reports, radar photographs and conventional weather analyses were used to complement the satellite data.

A computer program was utilized to accept Nimbus 2 HRIR equivalent blackbody temperatures (T_{BB} in °K) within historical maximum and minimum sea surface temperature limits over the tropical Atlantic Ocean. The sea surface temperatures maps resulting from the highest daily T_{BB} averages over 1° squares for a 10 day and 30 day period in September 1966 compared well with conventional and climatological oceanographic data in this sparse data region.

CONTENTS

THE DEVELOPMENT OF HURRICANE INEZ, 1966, AS SHOWN BY SATELLITE NIGHTTIME RADIOMETRIC AND DAYTIME TELEVISION COVERAGE

INTRODUCTION

With the development of long range international plans for the Global Atmospheric Research Program (GARP) and the GARP Tropical Atlantic Experiment (GATE) for the mid-1970's, there is an increasing scientific interest in studies of tropical cyclone formation in the Atlantic Ocean. (U. S. Committee for the GARP 1969, 1971, Zipser, 1969, De La Moriniere, 1972). Intensive investigation of convective cloud clusters (Martin and Suomi, 1972), surges in the Intertropical Zone of Convergence (ITC), westward moving waves from Africa, downward development of upper tropospheric vortices (cold lows) and baroclinic areas will be conducted in the Atlantic Ocean primarily between 5° N-15° N, 23°W-30° W and secondarily between 10° N-20° N, 47°W-54°W (ICSU/WMO Organizing Committee, 1971).

The unique life history of Hurricane Inez, 1966 was selected for this study because it moved through the above mentioned area as a wave which eminated from Africa, and developed through two distinct hurricane stages in the western Atlantic and Gulf of Mexico (Sugg and Carrodus, 1969). Nearly all of its 25 days of existence was well documented by Nimbus 2 nighttime satellite radiation data and ESSA 1 and 3 daytime television coverage, which are presented in the Appendix to this report. In addition, conventional meteorological analyses and satellite-derived sea surface temperatures were analyzed on a near-synoptic time scale.

Satellite television pictures resemble normal photographs and need no explanation; however, introductory remarks are necessary to interpret the nighttime Nimbus 2 High Resolution Infrared Radiometer (HRIR) data used in the re-report.

The Nimbus 2 High Resolution Infrared Radiometer (HRIR) Data

The Nimbus 2 High Resolution Infrared Radiometer is a single-channel scanning instrument sensitive in the 3. 5 to 4.2 micron "atmospheric window." The radiometer was designed to measure radiance temperatures between 210° K and 330° K with noise-equivalent temperature differences of 1° K for a 250° K background but for the period of this study, brightness values colder than 230° K which is the lower detection limit of the radiometer should be viewed with some reservation. A more complete discussion of the radiometer and satellite radiation data processing can be found in the Nimbus Project (1966), Warnecke et al. (1968).

Detailed observations of three-dimensional cloud structures are made possible at night by the small field of view of the radiometer which measures an average value of radiant energy from the earth's surface that is dependent on the nadir angle of the scan beam. At an average satellite altitude of 1100 kms, an 8.6 by 9.7 km area is viewed at the subsatellite point. The Nimbus 2 radiometer measurements differ from the ESSA 1 and 3 satellite television pictures shown in this report in that the radiometer measures outgoing emitted radiation while the television pictures depict differences in reflected solar radiation. In the absence of sunlight, blackbody radiation can be assumed and the detected radiance can be converted to the temperature of the radiating surface ("equivalent blackbody temperature, 'T_{BB}'"). This permits the derivation of earth or ocean surface temperatures, under clear sky conditions and cloud top heights when an opaque, plane cloud surface fills the field of view of the radiometer (Warnecke et al., 1969). When interpreting the measured equivalent blackbody temperature as cloud-top temperature, an approximate conversion of these values into cloud top height can be performed using the tropical atmosphere from the U. S. Standard Atmosphere Supplements (1966) for the temperature-height relationship. This relationship is used in the legend of the grid print map analyses of Nimbus 2 HRIR measurements shown in the Appendix.

The Nimbus 2 HRIR film strips used in this study are photographic images formed scan by scan on a photofacsimile machine from the original analog record of the data. No absolute values of either temperatures or temperature difference can be derived from the black and white tones in the pictures because reproductions from the original negatives were exposure controlled. An approximate geographic grid, accurate to within ±1 degree of great circle arc at the subsatellite point is superimposed upon the pictures for rough orientation.

The ten grid print maps analyzed in this study are a computer transformation of the radiation data into a standard mercator map projection with 0.625 degree longitude per grid interval. This map scale insures that 8 to 12 individual radiometer scan spots are averaged per grid square and thus provide an adequate data filter for background instrumental and electronic noise. A 50 degree scan nadir angle limit was used to permit a maximum of 75 km^2 area of the earth to be viewed without excessive limb darkening.

The Early Development of Hurricane Inez, 1966

Hurricane Inez, 1966 was classified by the National Hurricane Center, Miami, Florida as one of the "great" hurricanes of this century (Kraft, 1966). During its 15 days of sustained hurricane intensity in the Atlantic Ocean, Caribbean Sea and Gulf of Mexico, it left a path of devastation which totalled 1000 persons dead and $200 million dollars in property damage. It developed from a disturbance line which originated in the upper moist easterly monsoonal flow over the Sahara Desert (Sugg, 1967, Carlson, 1969 a, b). This type of perturbation normally moves westward at about 15 kts with the mean tropospheric wind between 600 and 700 mbs between 15° and 17° N and are observed to pass Dakar every third or fourth day (Carlson, 1969 (c)).

Figures A-1, -2, -3 shows our best estimate of the location of Inez in its early stages over west Africa from 15-17 September 1966. A time section of Dakar, Senegal (Figure A-4) indicates the passage on 18-19 September of a moist cloudy region which we believe was the northern edge of Inez as a wave, moving westward to the Atlantic from the Sahara.

The intense cloud band shown extending NE/SW from the Mediterranean Sea to 5° N in Figures A-2, -5, -7, -8 is related to a 300 mb trough which persisted off West Africa until 22 September, 1966 (Meteorologische Abhandlungen, 1966). Inez interacted with this high-level trough and by 20-21 September (Figures A-5, -6, -7, -8, -9, -10) exhibited the typical comma cloud form of a tropical depression as its circulation intensified. Figure A-9, indicates intense vertical cloud development on 21 September from 5 to over 11 km (270° to < 230° K) at 35° W, 10°-15° N.

Oceanographic Analyses of the Tropical Atlantic Ocean

In several articles, Carlson (1971, 1969 (a)) suggested that the frequency of tropical storm formation from African disturbances is dependent upon the Atlantic sea surface temperatures west of the African Coast. Based upon 66 years of tropical storm data, he showed the preferred region for tropical storm formation generated from African waves (Figure A-11). Note the cluster of initial storm positions from 40° W to 65° W, 10° N to 20° N near the 81.25° to 82.5° F isotherms.

Perlroth (1967, 1969) also supports this premise by showing that greater numbers of tropical storms reached hurricane intensity over oceanic areas where small (≤ 7°F) vertical temperature differences existed between the surface and 200 ft and the mixed layer was at least at the 100 to 250 ft depth level (Figure A-12). Inez started to develop as a depression on 21 September 1966 over the mean 100 ft mixed layer depth, in good agreement with the above discussion.

In order to determine the sea surface temperatures that existed prior and during the formation and development of Inez, all available conventional Atlantic Ocean 5-, 15-, 30-day mean sea surface temperature charts for September 1966 were obtained from the U. S. Navy Fleet Numerical Facility, Monterey, California. A computer program originally devised by LaViolette and Chabot

(1969) was utilized to derive sea surface temperature data during the same period. This program attempts to eliminate cloud contaminated scan spots by only accepting nighttime T_{BB} values that lie between historical maximum and minimum temperatures (±1° C) for 1° latitude-longitude squares in the area of interest (U. S. Naval Oceanographic Office, 1969). Only those T_{BB} values which were the highest daily average (HDA) in 1° squares for thirteen days (1-10, 13, 15, 16 September 1966) Figure A-13, and one month (1-30 September 1966) Figure A-14 were retained and analyzed. Prior to grid print map production, the Nimbus 2 meteorological radiation tapes (NMRT) were run through a mathematical filter produced by McMillin (1969) to reduce a residual oscillatory noise component. More recent papers by Braun, 1971 and Anding and Kauth, 1970 discuss the practical limits of the accuracy of infrared measurements of sea surface temperature from satellites.

The track of Inez was superimposed on Figures A-12 to -15 from aerial reconnaissance reports (Annual Tropical Storm Report, 1966) and coincident satellite data. An interesting oceanographic feature shown in the 13-day HDA chart at Point A in Figure A-13 is the southwestward penetration of the North Equatorial Current to 10° N, 52° W. This feature was also shown at Point B, 15°N, 48°W in the monthly (1-30 September 1966) HDA chart and is in good agreement with the conventional U. S. Navy sea surface temperature charts (Figure A-15) in the following features:

a. The area from Spain, southwestward off Africa show a decrease from 27°C to 20°C.

b. The area from 20° S off west Africa, northwestward to the tropical Atlantic show a decrease from 27°C to 15°C.

c. The area from west Africa 15° N to 5° N westward to the Gulf of Mexico show the gradual increase in the 28°, 29° and 30° C isotherms.

Persistent cloudy regions which are indicated by cold T_{BB} readings are shown by diagonal lines in the HDA charts.

The addition of 1° to 2.5° C was needed to correct the HDA sea surface temperature values for water vapor and carbon dioxide absorption, micro-surface effect, emissivity effect, and minor constituent absorption (Warnecke et al., 1969, 1971). This result compares well with 1.5° to 2.6°C RMS differences between ship and satellite measurements described in other more rigorous statistical techniques using HRIR data (Smith et al., 1970, Smith and Rao, 1971, Arnold et al., 1971, Greaves et al., 1968, Curtis and Rao, 1969, Rao et al., 1971, Szekielda et al., 1970, Vukovich 1970 and multispectral techniques using

Nimbus 2 Medium Resolution Infrared Radiometer (MRIR) data by Shenk and Salomonson, 1970.

The Later Development of Hurricane Inez, 1966

Tropical Depression Inez continued to move northwesterly on 22 September (Figures A-16, -17). On 23 September (Figures A-18, -19) the cirrus canopy rounded out to fill a 5° latitude circle just as a 300 mb trough approached from the west. This type of cloud "blow up" or expansion had been previously described by Frank (1969). Inez gradually developed into a tropical storm on 24 September (Sugg, 1967) (Figure A-20). This intensification occurred close to the 28° C sea surface isotherm near 10° N-15° N, 40° W-50° W (Figure A-13) and under the positive influence of the semi-permanent high level ridge.

Figure A-21 depicts a "dynamic profile" of Inez from September 24 - October 11, 1966 in which the smoothed maximum surface winds (kts) and smoothed surface pressure (mbs) show two distinct hurricane stages. The first stage occurred in the western Atlantic, the second in the Gulf of Mexico (U. S. Dept. of Commerce, 1966 (a) and (b)). Inez continued to move on a northwesterly course at a slower forward speed on 25 September (Figures A-22, -23) and reached hurricane intensity on 26 September (Figure A-24). It then continued on a westnorthwestward track and intensified on the periphery of the subtropical Bermuda High. The center of the hurricane moved almost directly over Guadaloupe on 27 September (Figures A-25 and A-27). Hurricane Inez had a small cloud canopy, approximately 3.5° in diameter, as shown by the T_{BB} analysis in Figure A-26. Hawkins and Rubsam (1969) classified Inez as a micro-hurricane on 28-29 September because of its characteristic small, tight cloud structure and strong maximum surface wind ($>$ 130 knots) and low ($<$ 927 mb) surface pressure. Hubert et al., 1969 included the "atypical" Inez in his calculation of the maximum wind speed from the degree of hurricane organization, canopy size (using the 260 T_{BB} isotherm) and inner eye wall radius.

Tropical Storm Judith which developed and dissipated during the same period, 28-30 September, is shown in great detail in Figures A-28, A-29, A-33 and A-34. Note that Judith's cloud canopy gradually increased to twice the size of the Inez canopy ($<$ 260°K T_{BB} value) by 30 September, the day when it finally degenerated into an easterly wave (U. S. Dept. of Commerce, 1966 (b)). Time sections for Antigua, British West Indies, and San Juan, Puerto Rico were plotted in Figures A-35 and A-36. They confirm that the narrow cloud region of Inez is shown by the 40% to 60% relative humidity isopleths reached from 250 to 190 mbs (33,000 to 40,000 ft). This generally agrees with the $>$ 230° K T_{BB} values for the high level cirrus canopy clouds shown in Figures A-26, A-29, A-30, A-31 and A-32. One to four degree C warming indicated the warm core of the storm at the 200 to 350 mb level. Deep layers of dry air (20% relative humidity down to the 700 mb level) implies strong subsidence prior to and following Inez passage through the area. Anticyclonic outflow above 200 mb is accompanied by northwesterly to southwesterly winds while lower level inflow winds are from the easterly quadrant.

The hurricane's intensity started to diminish from 29 September on to 2 October, as Inez was affected by the mountainous terrain of Haiti and the Dominican Republic (Herbert, 1967). The Sierra Maestra Mountains in eastern Cuba left Inez weak and disorganized and the tropical storm turned northward through central Cuba by October 1. Figures A-37, A-38, and A-39 show the elongated northwest to southeast orientation of the distorted cloud field with weak cirrus outflow aloft.

Moving north-northeastward into the Florida Straits, Inez regenerated hurricane strength winds late on 2 October and spawned a tornado over Nassau. The hurricane continued to intensify and a radar picture of the diffuse 30-40 mile wide eye of Inez was recorded by Miami radar at midnight 2 October (Figure A-40).

A combined radar track from Key West and Miami radar stations and satellite nighttime radiation-television coverage of Inez from 2-6 October 1966 is shown in Figures A-40, A-41 to A-47.

Inez had been forecast to continue its path to the northeast around the Bermuda High. However, it moved just east of Bimini Island, (100 miles east of Miami) and stalled by noon of 3 October. The hurricane's erratic surface positions were recorded by Miami radar and is shown between 78° to 79°W, 25° to 26°N (Figure A-46). The lack of intensification appeared to be related to a weak upper-level trough on 3 October. However, a trend to the west-southwest was established on the 4th of October 1966. Figure A-48 shows the 00GMT, 300 mb chart for 4 October which was typical of the upper air flow of the region until 9 October 1966. A strong anticyclone had formed over the central Gulf of Mexico and Inez was steered around its southern edge. A time section at Miami, Florida (Figure A-49) shows the deep layer of dry air ($<$ 40% R. H. from 600-700 mb to 250 mb) from 3 to 7 October, which is related to the subsidence from the eastern portion of the upper level high in the Gulf of Mexico. Inez moved over the Florida Keys, intensified and brushed Merida on the north coast of Yucatan on 7 October (Figures A-50, A-51 and A-52). A time section at Merida, Mexico (Figure A-14) shows the increase in height of the 40% R.H. isopleth to 250 mb and the 230° T_{BB} values (cirrus canopy in Figure A-53) to 11 km.

The ridge aloft over the Gulf weakened and permitted Inez to drift northwestward and westward on the 8th and 9th of October (Figures A-54 to A-58), until it reached the Mexican coast north of Tampico on the 10th of October. (A-59 to A-61). Tampico reported gusts to 127 mph and torrential rains which caused widespread flood in the area. By 11 October, the storm had lost its energy after it passed inland over the mountainous terrain in Mexico (DeAngelis, 1967).

CONCLUSIONS

The chronological study of the growth and development of a tropical cyclone utilizing 12-hour continuity from satellite radiation and television data and conventional meteorological analyses has shown the unique advantages of satellite remote sensing techniques. The Advanced Technology satellites (ATS F and G) and Synchronous Meteorological satellites (SMS) will be equipped with radiometers and will make available on an operational and research basis 20-minute, 24-hour a day full earth disc coverage of tropical and mid-latitude cloud development and sea surface temperature measurements in cloud-free regions. These sensors should open up a new dimension in tropical cyclone and oceanographic research during the 1973-75 period.

ACKNOWLEDGEMENTS

The author would like to thank Dr. Raymond Wexler for his helpful comments and suggestions in the review of this paper. I am particularly grateful to Mr. Joseph Steranka and Mark Smith, for their assistance in the time cross-sections and satellite radiation analyses, to the National Environmental Satellite Service, NOAA, Washington, D.C. for providing the ESSA 1 and 3 satellite television pictures and to Mr. Paul LaViolette, NOAA for his extensive support in the analysis of the tropical Atlantic satellite-derived sea surface temperature data.

REFERENCES

Anding, D. and R. Kauth, 1970: "Estimation of Sea Surface Temperature from Space," Remote Sensing of Environment, Vol. 1, No. 4, New York, N.Y., Dec. 1970, pp. 217-220.

Annual Tropical Storm Report - 1966, U. S. Fleet Weather Facility, Jacksonville, Florida. OPHAU Report 3140-9, 15 April 1967, pp. II-64 to 73.

Arnold, J. E., A. H. Thompson and L. Y. Chen, 1971: "Statistical Evaluations of Sea Surface Temperature Distributions Based Upon Nimbus Satellite HRIR Data," Final Report, Texas A&M Research Foundation, College Station, Texas, pp. 111.

Braun, C., 1971: "Limits on the Accuracy of Infrared Radiation Measurements of Sea Surface Temperature from a Satellite," NOAA Technical Memorandum NESS 30, Wash., D.C., pp. 28.

Carlson, T. N., 1969(a): "Some Remarks on African Disturbances and Their Progress Across the Tropical Atlantic," Monthly Weather Review, Vol. 97, No. 10, pp. 716-726.

Carlson, T. N., 1969(b): "Hurricane Genesis from Disturbances Formed Over Africa," Mariners Weather Log, Vol. 13, No. 5, pp. 197-202.

Carlson, T. N., 1969(c): "Synoptic Histories of Three African Disturbances That Developed into Atlantic Hurricanes," Monthly Weather Review, Vol. 97, No. 3, pp. 256-276.

Carlson, T. N., 1971: "An Apparent Relationship Between the Sea Surface Temperature of the Tropical Atlantic and the Development of African Disturbances into Tropical Storms," Monthly Weather Review, Vol. 99, No. 4, pp. 309-310.

Curtis, W. R. and P. K. Rao, 1969: "Gulf Stream Thermal Gradients from Satellite, Ship and Aircraft Observations," Journal of Geophysical Research, Vol. 74, No. 28, pp. 6984-6990.

De Angelis, R. M., 1967: "North Atlantic Tropical Cyclones, 1966," Mariners Weather Log, Vol. 11, No. 1, U.S. Dept. of Commerce, ESSA EDS, pp. 10-16.

De La Moriniere, T., 1972: "BOMEX Temporary Archive Description of Available Data," NOAA Technical Report EDS 10, U.S. Dept. of Commerce, pp. 304.

Frank, N., 1969: "The Inverted V Cloud Pattern - An Easterly Wave," Monthly Weather Review, Vol. 97, No. 2, pp. 130-140.

Greaves, J. R., J. H. Willand, and D. T. Chang, 1968: "Observations of Sea Surface Temperature Patterns and Their Synoptic Change Through Optimal Processing by Nimbus 2 Data," Final Report, NASA Contract NASW-1651, Allied Research Associates, Concord, Mass., pp. 121.

Hawkins, H. F. and D. T. Rubsam, 1967: "Hurricane Inez - A Classic Micro-Hurricane," Mariners Weather Log, Vol. 11, No. 5, U. S. Dept. of Commerce, ESSA, EDS, pp. 157-160.

Herbert, P. J., 1967: "The Hurricane Season of 1966," Weatherwise, Vol. 20, No. 1, pp. 17-32.

Hubert, L. F., A. Timchalk and S. Frtiz, 1969: "Estimating Maximum Wind Speed of Tropical Storms from High Resolution Infrared Data," National Environmental Satellite Center, NESC, 50, pp. 33.

ICSU/WMO Organizing Committee, 1971: Report of the Fifth Session of the Joint Organizing Committee, Bombay, India.

Kraft, R. H., 1966: "Great Hurricanes, 1955-1965," Mariners Weather Log, Vol. 10., No. 6, U. S. Dept. of Commerce, ESSA, EDS, pp. 200-202.

LaViolette, P. E. and P. L. Chabot, 1969: "A Method of Eliminating Cloud Interference in Satellite Studies of Sea Surface Temperature," Deep Sea Research, Vol. 16, pp. 539-547.

Martin, D. W. and V. E. Suomi, 1972: "A Satellite Study of Cloud Clusters Over the Tropical North Atlantic Ocean," Bulletin of the American Meteorological Society, Vol. 53, No. 2, pp. 135-156.

McMillin, L. M., 1969: "A Procedure to Eliminate Periodic Noise Found in Nimbus 2 High Resolution Infrared Radiometer Measurements, NASA Contractor Report 9G45-32, pp. 16.

Meorologische Abhandlungen, 1966: "Tagliche Und Mittlere Boden-und 300-mb-Karten der Nordhemisphare, Sept. 1966, Band LXIV, Heft 9 Institut Fur Meteorologie und Geophysik der Frien, Universitat Berlin, W. Germany.

Nimbus Project, "Nimbus II Users' Guide," Goddard Space Flight Center, Greenbelt, Md., 1966.

Perlroth, I., 1967: "The Distribution of Water Type Structure in the First 300 Feet of the Equatorial Atlantic," National Oceanographic Data Center, P-6J, Washington, D. C., pp. 17.

Perlroth, I., 1969: "Effects of Oceanographic Media on Equatorial Atlantic Hurricanes," Tellus XXI, No. 2, pp. 230-244.

Rao, P. K., A. E. Strong and R. Koffler, 1971: "Sea Surface Temperature Mapping off the Eastern U. S. Using NASA's ITOS Satellite," Proceedings of the 7th International Symposium on Remote Sensing of Environment, Vol. 1, 17-21 May 1971, pp. 683-691.

Shenk, W. E. and V. V. Salomonson, 1970: "A Multispectral Technique to Determine Sea Surface Temperature Using Nimbus 2 Data," presented at the 1970 Fall AGW Meeting, San Francisco, California.

Smith, W. L., P. K. Rao, R. Koffler, and W. R. Curtis, 1970: "The Determination of Sea Surface Temperature from Satellite High Resolution Infrared Window Radiation Measurements," Monthly Weather Review, Vol. 98, No. 8, pp. 604-611.

Smith, W. L. and P. K. Rao, 1971: "Sea Surface Temperature Measurements from Satellites," presented at the 5th Symposium on Temperature, Its Measurement and Control, Science and Industry, June 21-24, 1971, Wash., D.C.

Sugg, A. L., 1967: "The Hurricane Season of 1966," Monthly Weather Review, Vol. 95, No. 3, U. S. Dept. of Commerce, ESSA, pp. 131-142.

Sugg, A. L. and Carrodus, R. L., 1969: "Memorable Hurricanes of the United States Since 1873," ESSA Tech. Memo. WBTM SR-42, pp. 50.

Szekielda, K. H., V. V. Salomonson and L. J. Allison, 1970: "Seasonal Sea Surface Temperature Variations in the Persian Gulf as recorded by Nimbus 2 HRIR," NASA X-651-70-416, Nov. 1970, Goddard Space Flight Center, Greenbelt, Md., pp. 14.

U. S. Committee for the Global Atmospheric Research Program, 1969: Plan for U. S. Participation in the Global Atmospheric Research Program, National Academy of Sciences, Washington, D. C.

U. S. Committee for the Global Atmospheric Research Program, 1971: Plan for U. S. Participation in the GARP Atlantic Tropical Experiment, National Academy of Sciences, Washington, D. C.

U. S. Dept. of Commerce, ESSA, Weather Bureau, 1966(a): Hurricane Inez - Sept. 21 - Oct. 10, 1966, Preliminary Reports with Advisories and Bulletins issued," Wash. D. C., pp. 64.

U. S. Department of Commerce, 1966(b): Rough Log, North Atlantic Weather, July - September 1966, Mariners Weather Log, Vol. 10, No. 6, Nov. 1966, pp. 219-221.

U. S. Naval Oceanographic Office, 1969: Mean Maximum and Minimum September Sea Surface Temperature Data, Atlantic Ocean, Wash., D. C.

U. S. Standard Atmosphere Supplements, 1966: ESSA, NASA, U. S. Air Force, Supt. of Documents, U. S. Government Printing Office, Wash., D. C. 20402.

Vukovich, F. M., 1970: "Physical Oceanography Feasibility Study Utilizing Satellite Data: Part II, Detailed Sea Surface Temperature Analysis Utilizing Nimbus HRIR Data," Final Report, Contract E-236-69(N), Research Triangle Institute, Research Triangle Park, North Carolina.

Warnecke, G., L. J. Allison, E. R. Kreins and L. M. McMillin, 1968: "A Satellite View of Typhoon Marie 1966 Development," NASA Technical Note D-4757, pp. 94.

Warnecke, G., L. M. McMillin and L. J. Allison, 1969: "Ocean Current and Sea Surface Temperature Observations from Meteorological Satellites," NASA Technical Note D-5142, pp. 47.

Warnecke, G., L. J. Allison, L. M. McMillin and K. H. Szekielda, 1971: "Remote Sensing of Ocean Currents and Sea Surface Temperature Changes Derived from the Nimbus 2 Satellite," Journal of Physical Oceanography, Vol. 1, No. 1, pp. 45-60.

Zipser, E. J., 1969: "Survey of Progress and Plans in Tropical Meteorological Experiments," Air Weather Service Technical Report 217, AWS (MAC), U. S. Air Force, Scott AFB, Ill., pp. 178-188.

APPENDIX

SATELLITE NIGHTTIME RADIOMETRIC AND DAYTIME TELEVISION COVERAGE AND CONVENTIONAL METEOROLOGICAL ANALYSES

APPENDIX

FIGURE CAPTIONS

Figure A-1. ESSA 1 television photograph (orbit 3218) on September 15, 1966 at 1422 GMT.

Figure A-2. Nimbus 2 HRIR film strip (orbit 1647) on September 16, 1966, near 0100 GMT.

Figure A-3. ESSA 1 television photograph (orbit 3247) on September 17, 1966 at 1452 GMT.

Figure A-4. Time section (00 GMT) at Dakar, Senegal from 10-26 Setpember 1966. Gray tone areas show region of 0° to 5° temperature - dewpoint differences (increased moisture content).

Figure A-5. Nimbus 2 HRIR film strip (orbit 1687) on September 19, 1966, near 0100 GMT.

Figure A-6. ESSA 1 television photograph (orbit 3276) on September 19, 1966 at 1523 GMT.

Figure A-7. Nimbus 2 HRIR film strip (orbit 1700) on September 20, 1966, near 0100 GMT.

Figure A-8. Nimbus 2 HRIR film strip (orbit 1714) on September 21, 1966, near 0200 GMT.

Figure A-9. Analysis of Nimbus 2 HRIR measurements (orbit 1714) on September 21, 1966 near 0200 GMT (near local midnight) based upon a computer grid print map with 0.625 degree longitude per grid interval.

Figure A-10. ESSA 1 television photograph (orbit 3305) on September 21, 1966 at 1550 GMT.

Figure A-11. Mean Sea Surface Isotherms for September in the Tropical Atlantic Ocean and Initial Positions of Tropical Storms, 1901-1967 (Carlson, 1969).

Figure A-60. Analysis of Nimbus 2 HRIR measurements (orbit 1969) on October 10, 1966 near 0600 GMT (near local midnight) over Hurricane Inez. This chart was based upon a computer grid print map with 0.625 degree longitude per grid interval.

Figure A-61. ESSA 3 television photograph (orbit 0105) on October 10, 1966 at 2038 GMT over Hurricane Inez.

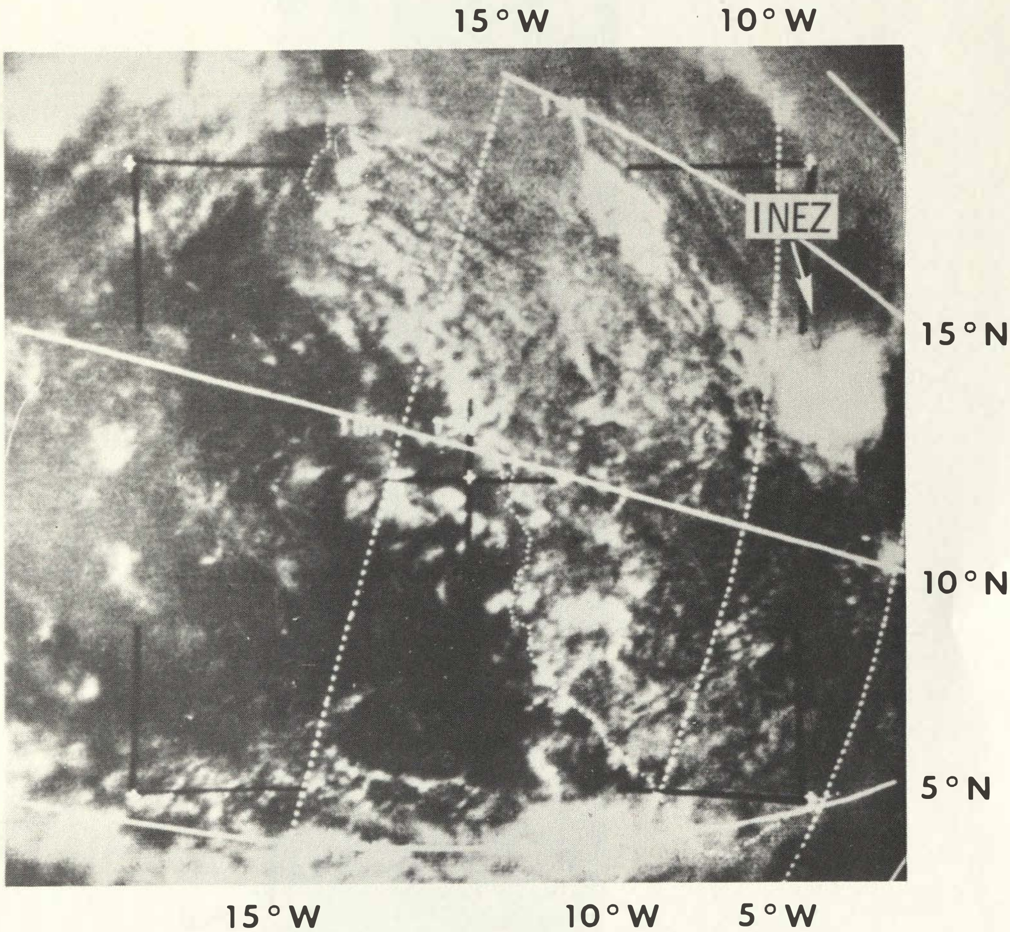

ESSA 1 ORBIT 3218 1422 Z

SEPT. 15, 1966

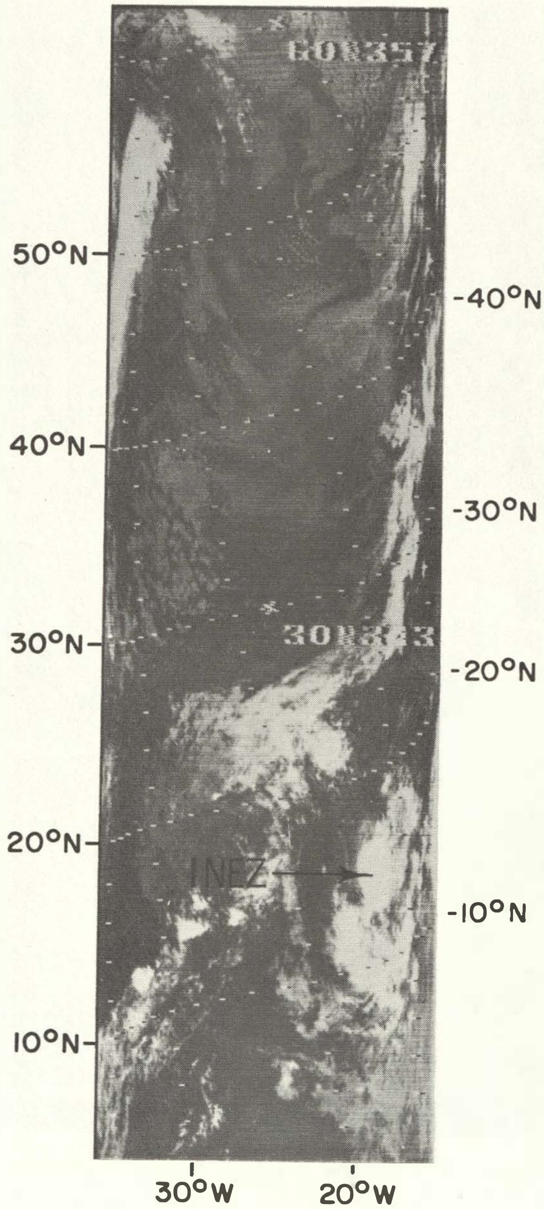

FORMATIVE STAGE
INEZ 1966
NIMBUS II HRIR
SEPT. 16, 1966

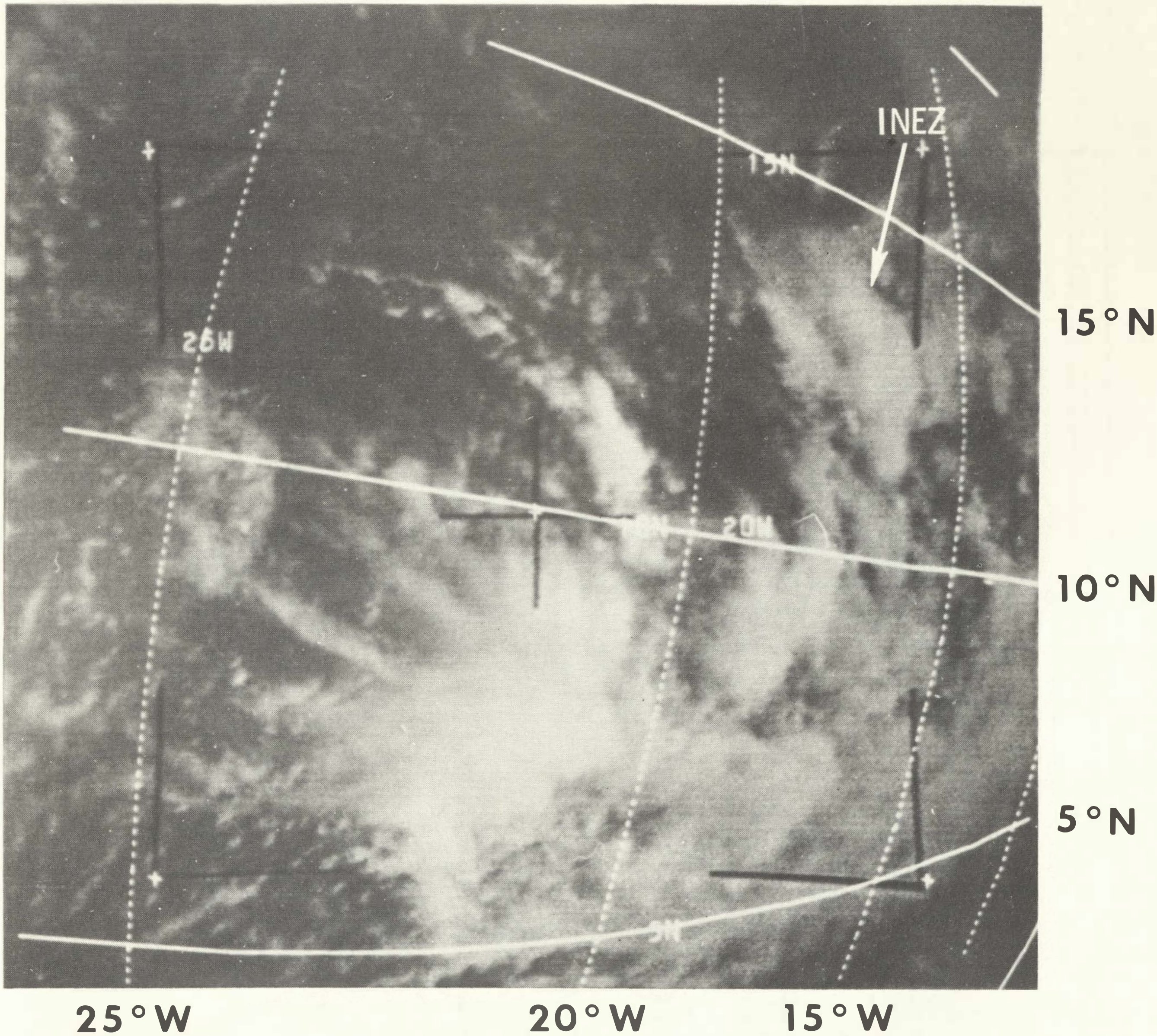

ESSA 1 ORBIT 3247 1452 Z

SEPT. 17, 1966

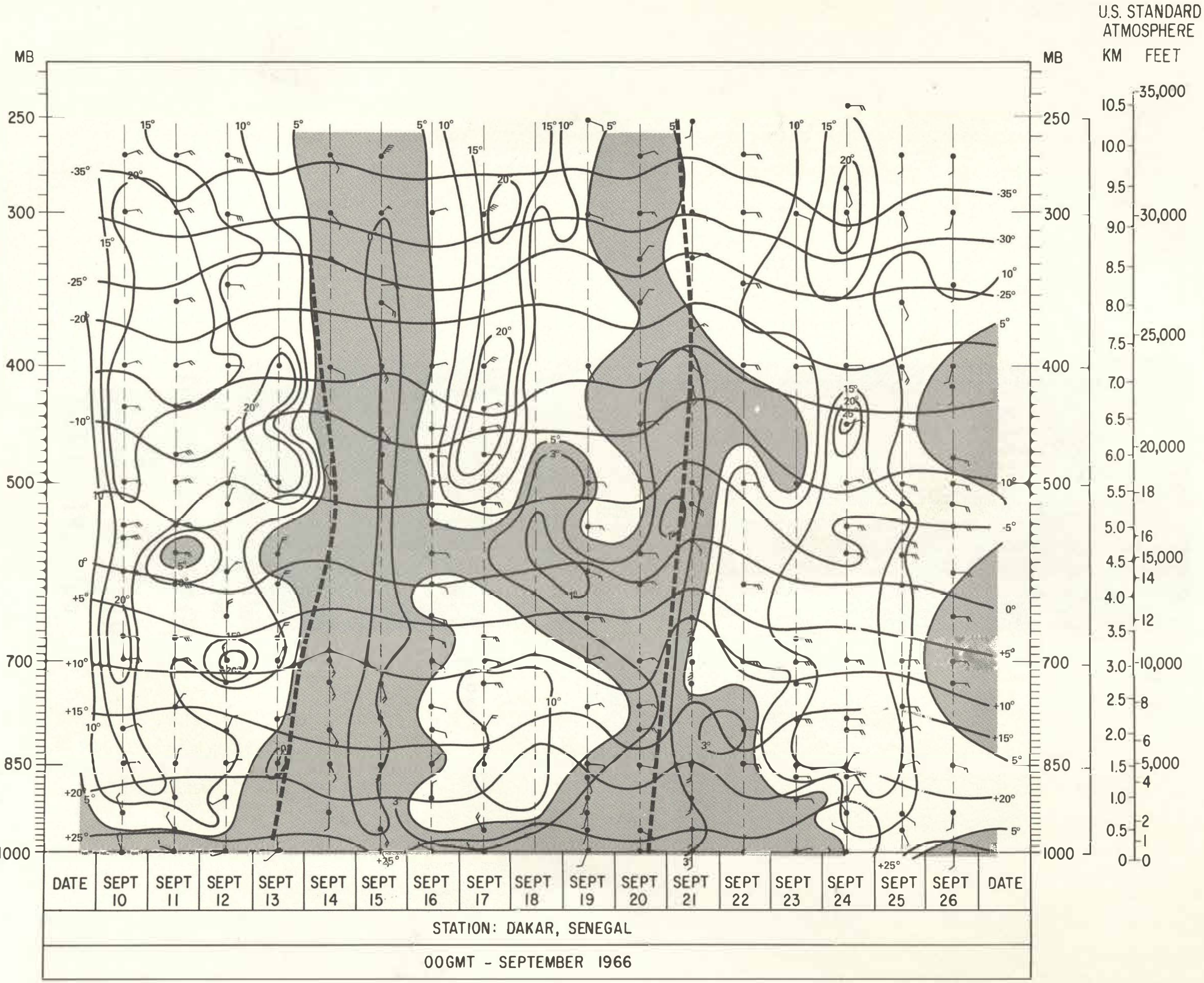
U.S. STANDARD ATMOSPHERE
KM FEET
MB
250
300
400
500
700
850
1000
DATE
SEPT 10
SEPT 11
SEPT 12
SEPT 13
SEPT 14
SEPT 15
SEPT 16
SEPT 17
SEPT 18
SEPT 19
SEPT 20
SEPT 21
SEPT 22
SEPT 23
SEPT 24
SEPT 25
SEPT 26
DATE
STATION: DAKAR, SENEGAL
00GMT - SEPTEMBER 1966

Figure A-4

FORMATIVE STAGE
INEZ 1966
NIMBUS II HRIR
SEPT. 19, 1966

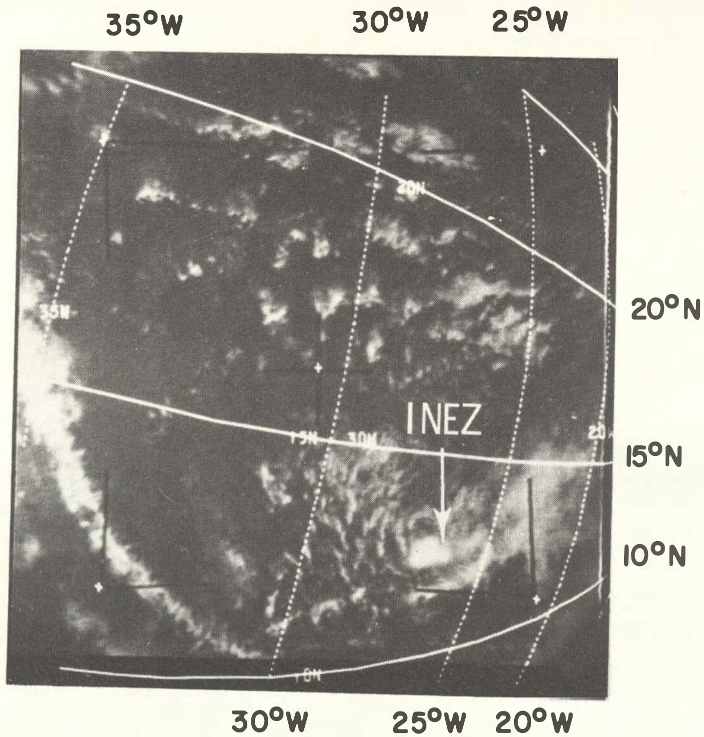

FORMATIVE STAGE
INEZ 1966
ESSA-I TV
SEPT. 19, 1966

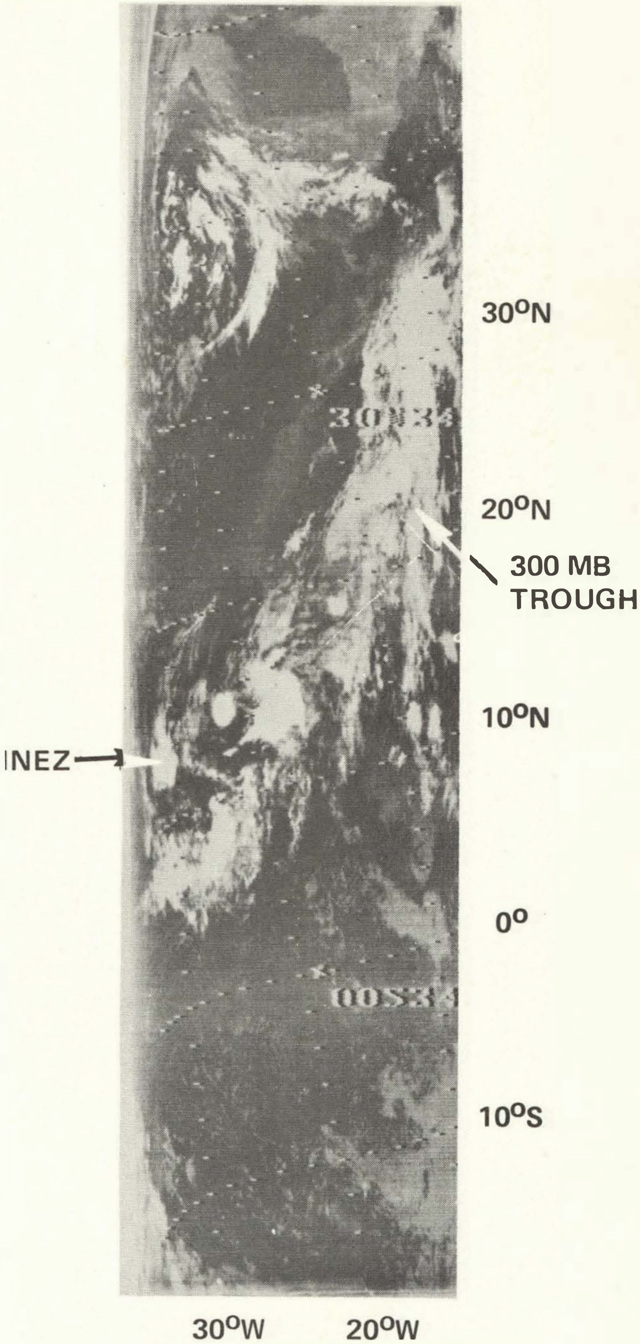

FORMATIVE STAGE
INEZ 1966
NIMBUS II HRIR
SEPT. 20, 1966

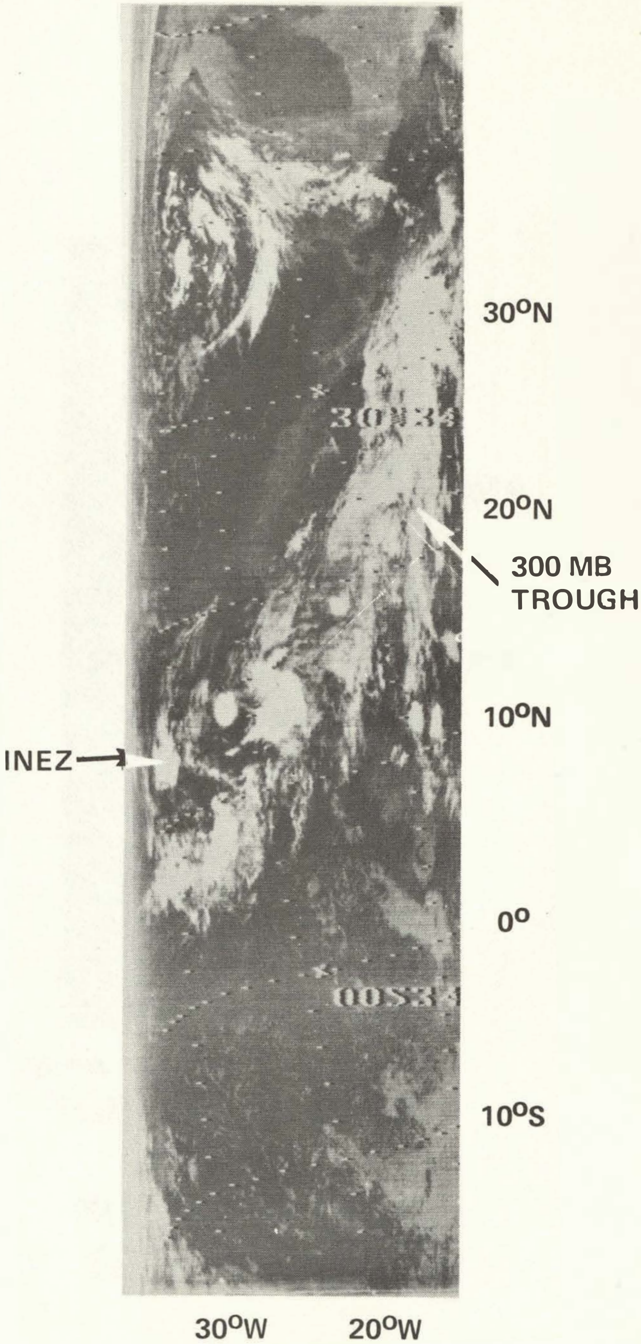

FORMATIVE STAGE
INEZ 1966
NIMBUS II HRIR
SEPT. 20, 1966

FORMATIVE STAGE
INEZ 1966
NIMBUS II HRIR
SEPT. 21, 1966

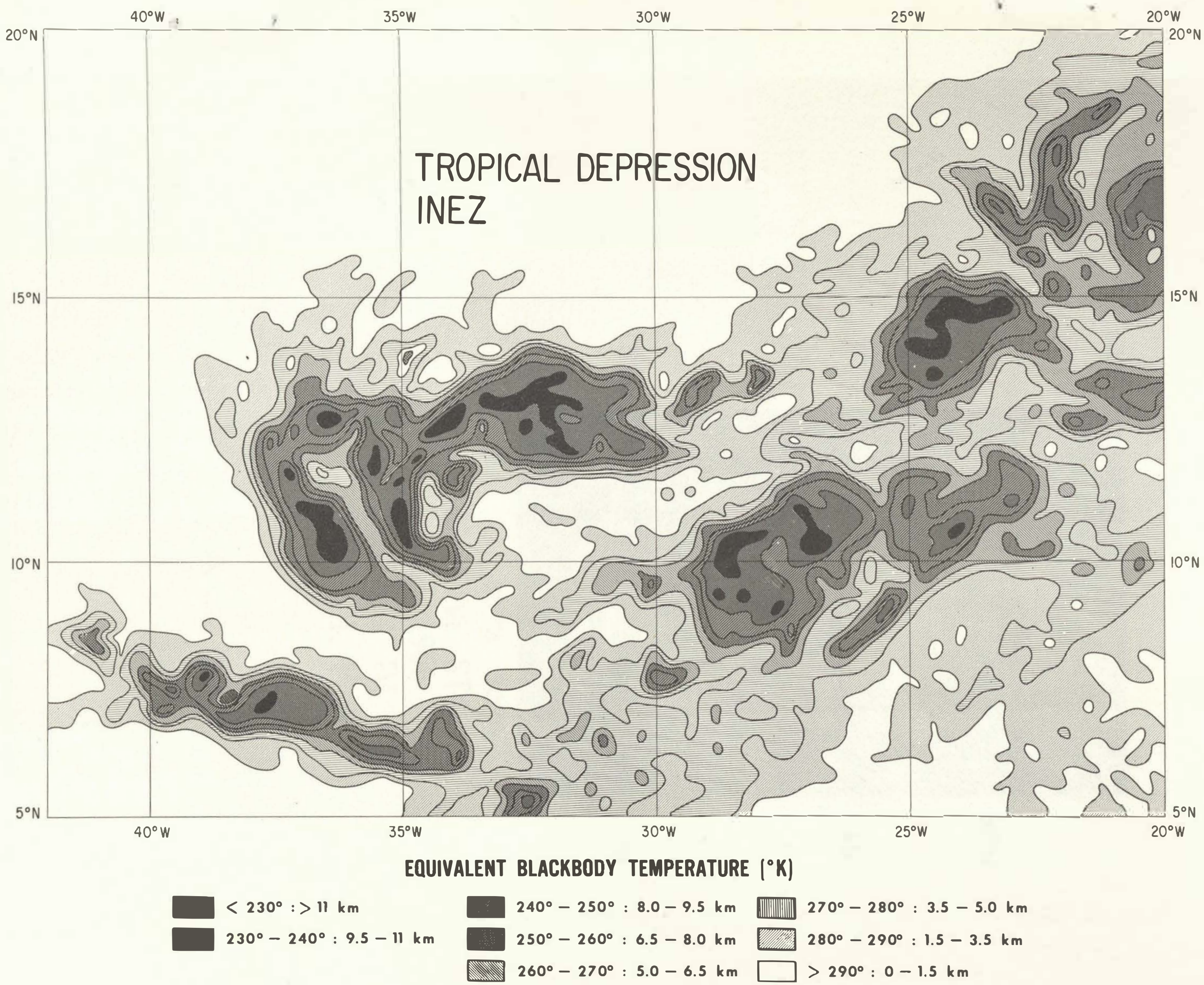

TROPICAL DEPRESSION INEZ, 1966

NIMBUS II HRIR

SEPTEMBER 21, 1966

Figure A-9

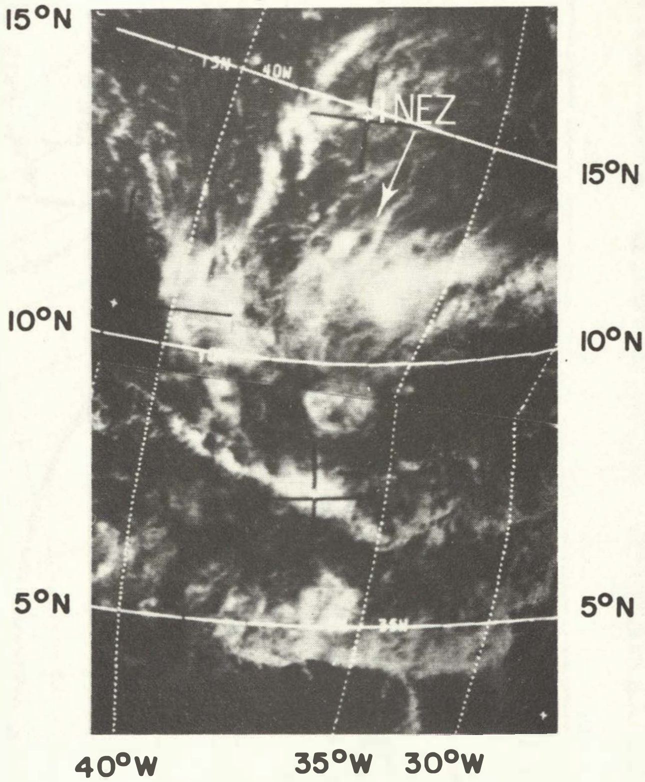

FORMATIVE STAGE
INEZ 1966
ESSA I TV
SEPT. 21, 1966

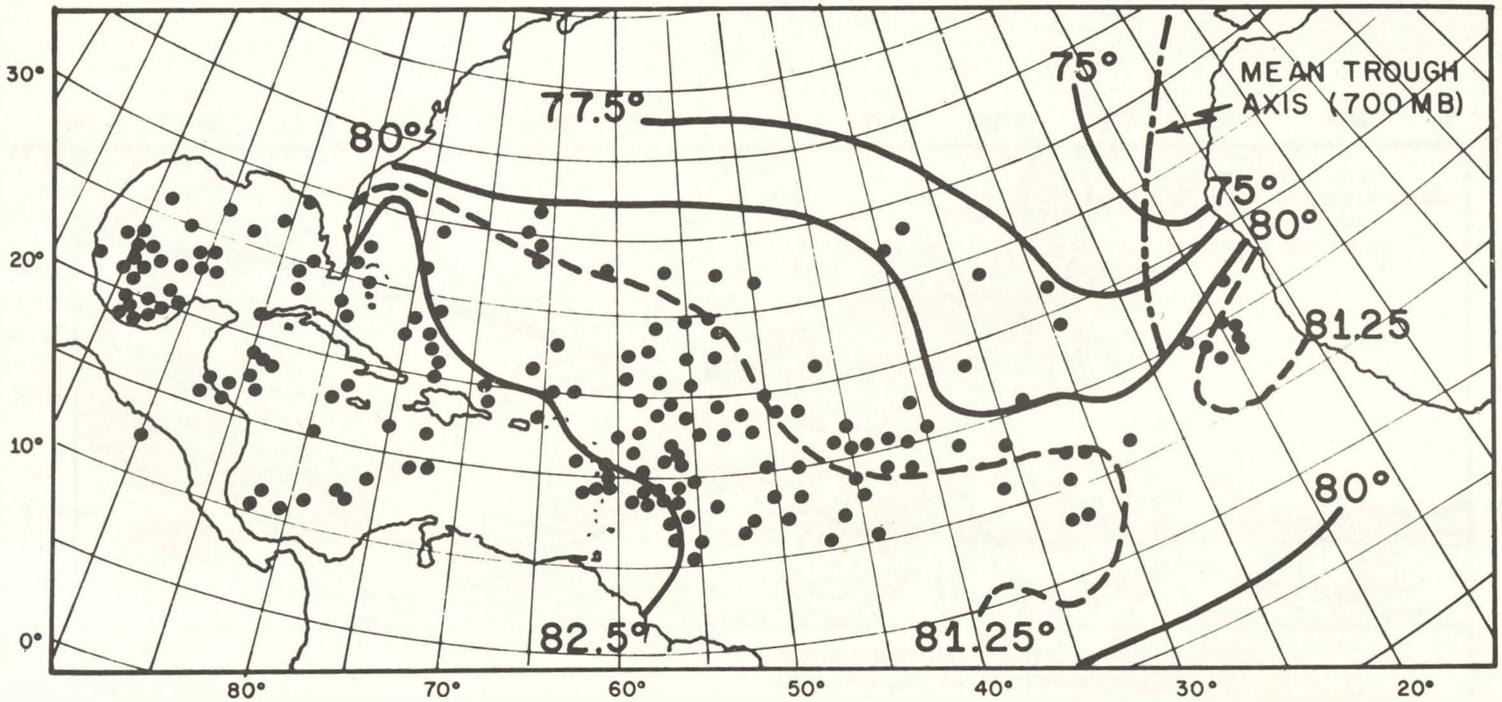

MEAN SEA SURFACE ISOTHERMS, SEPTEMBER, AND INITIAL POSITIONS OF TROPICAL STORMS, 1901 – 1967 — (CARLSON, 1969)

Figure A-11

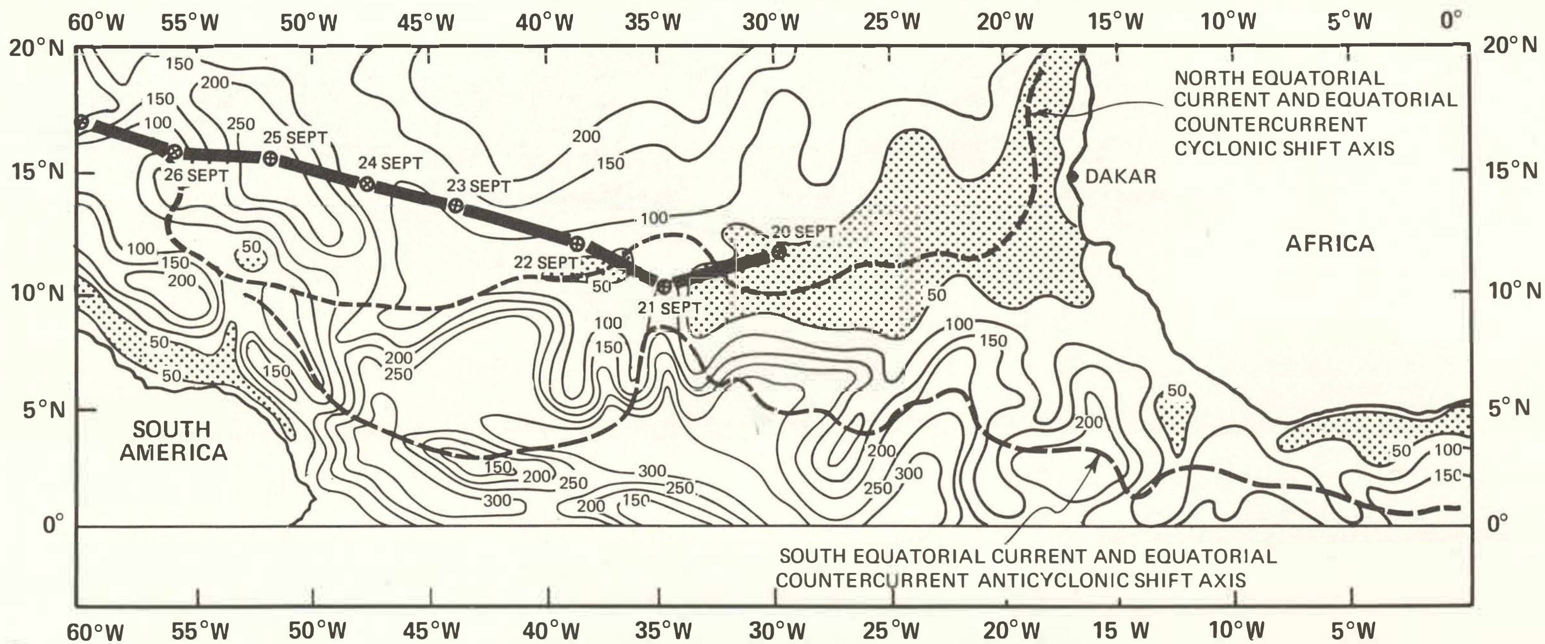

NORTH EQUATORIAL CURRENT AND EQUATORIAL COUNTERCURRENT CYCLONIC SHIFT AXIS
SOUTH EQUATORIAL CURRENT AND EQUATORIAL COUNTERCURRENT ANTICYCLONIC SHIFT AXIS
DAKAR
AFRICA
SOUTH AMERICA
20 SEPT
21 SEPT
22 SEPT
23 SEPT
24 SEPT
25 SEPT
26 SEPT
60°W
55°W
50°W
45°W
40°W
35°W
30°W
25°W
20°W
15°W
10°W
5°W
0°
20°N
15°N
10°N
5°N

Figure A-12

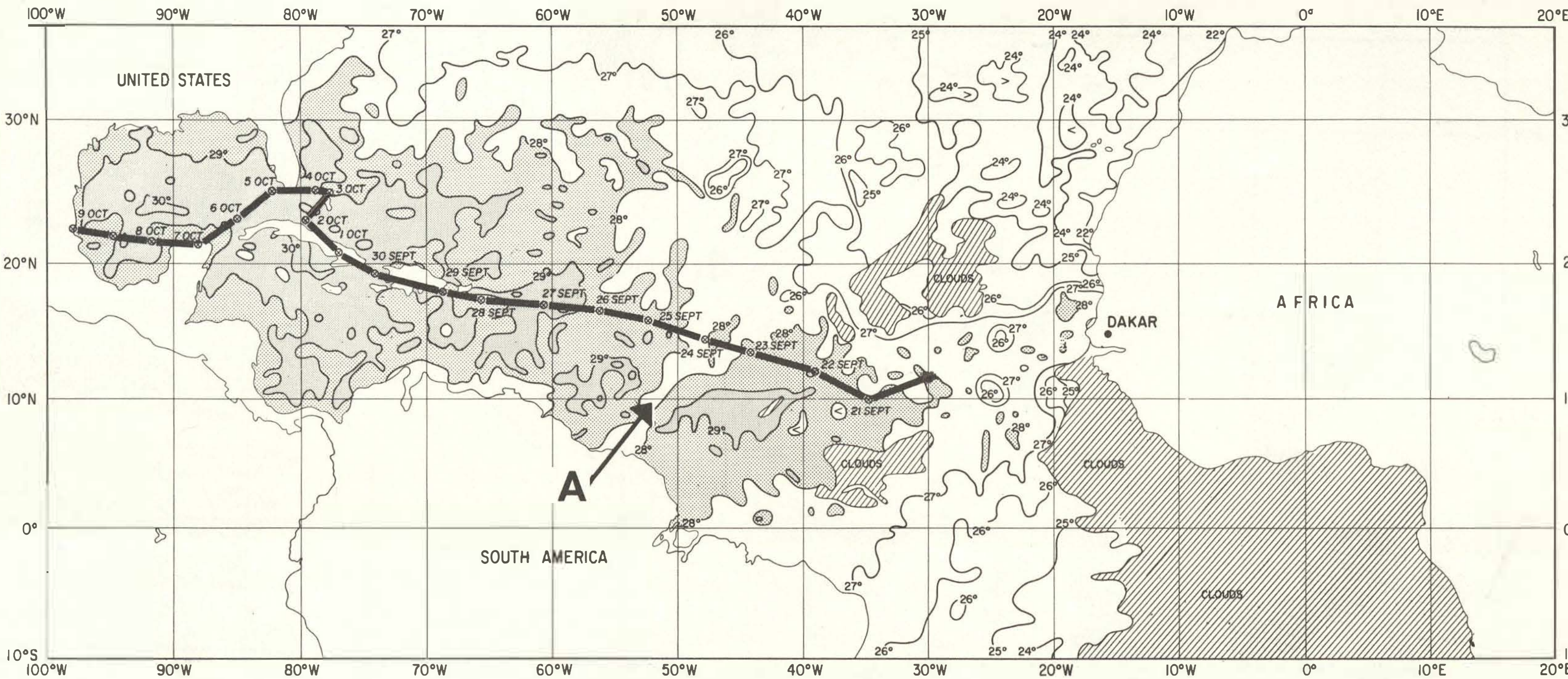

SEA SURFACE TEMPERATURES (°C)
DERIVED FROM NIMBUS II HRIR (HDA)
SEPT 1-10, 13, 15, 16, -1966

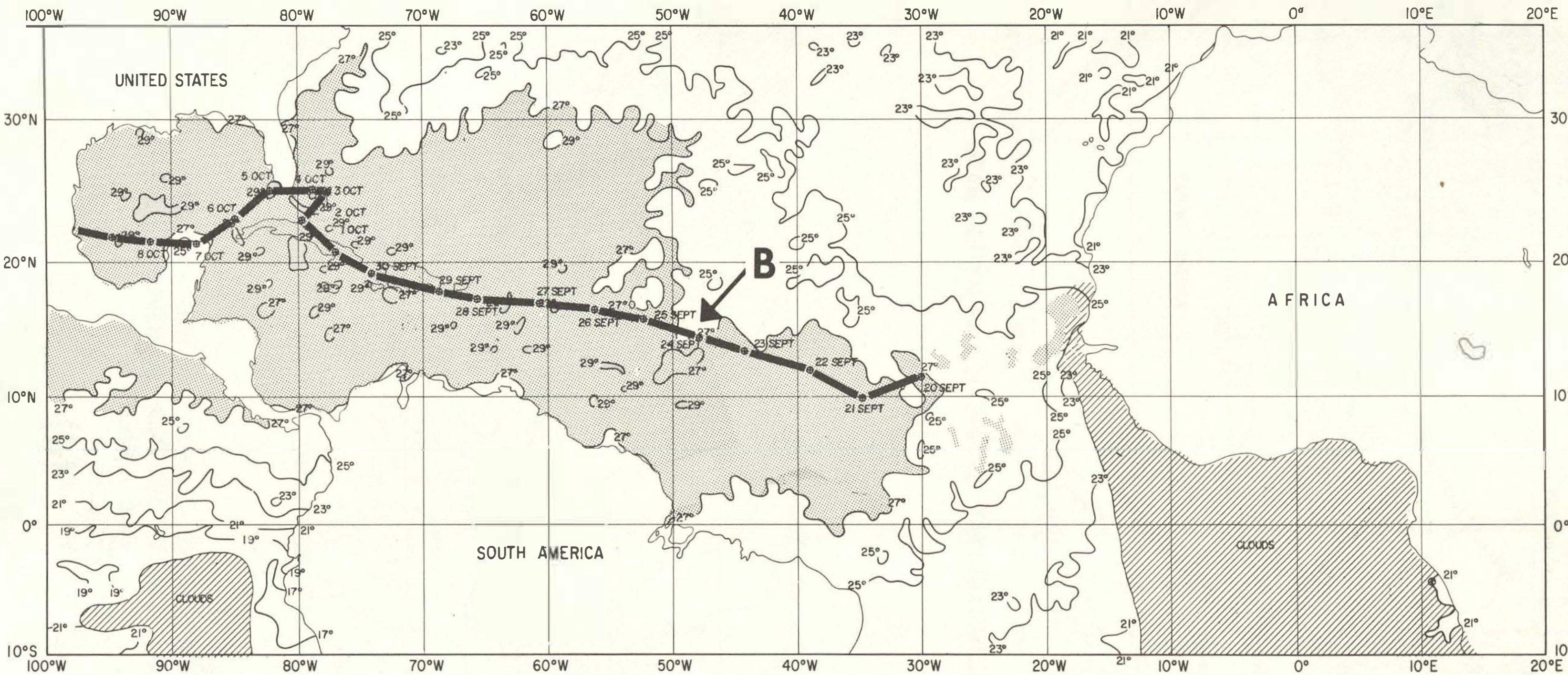

MONTHLY SEA SURFACE TEMPERATURES (°C)
DERIVED FROM NIMBUS II HRIR (HDA)
SEPT. 1-30, 1966

A — 14

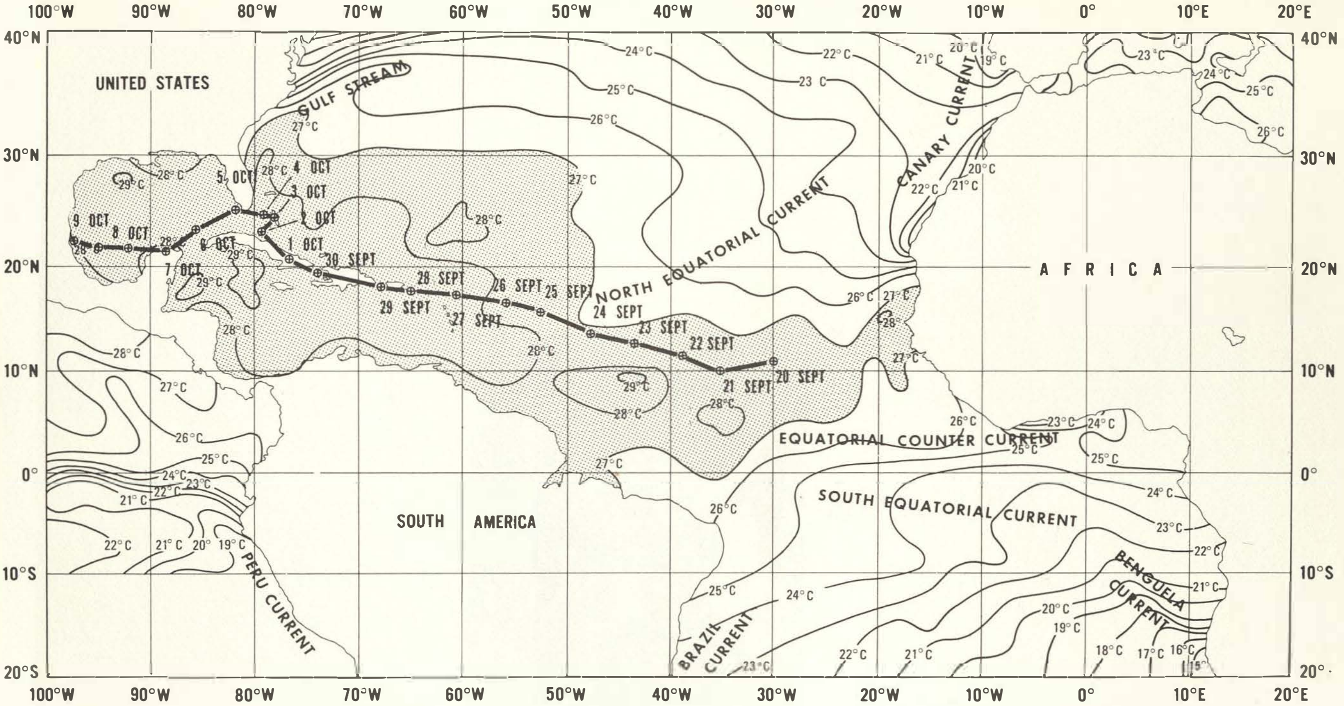

MEAN SEPTEMBER SEA SURFACE TEMPERATURES (°C)

(a)

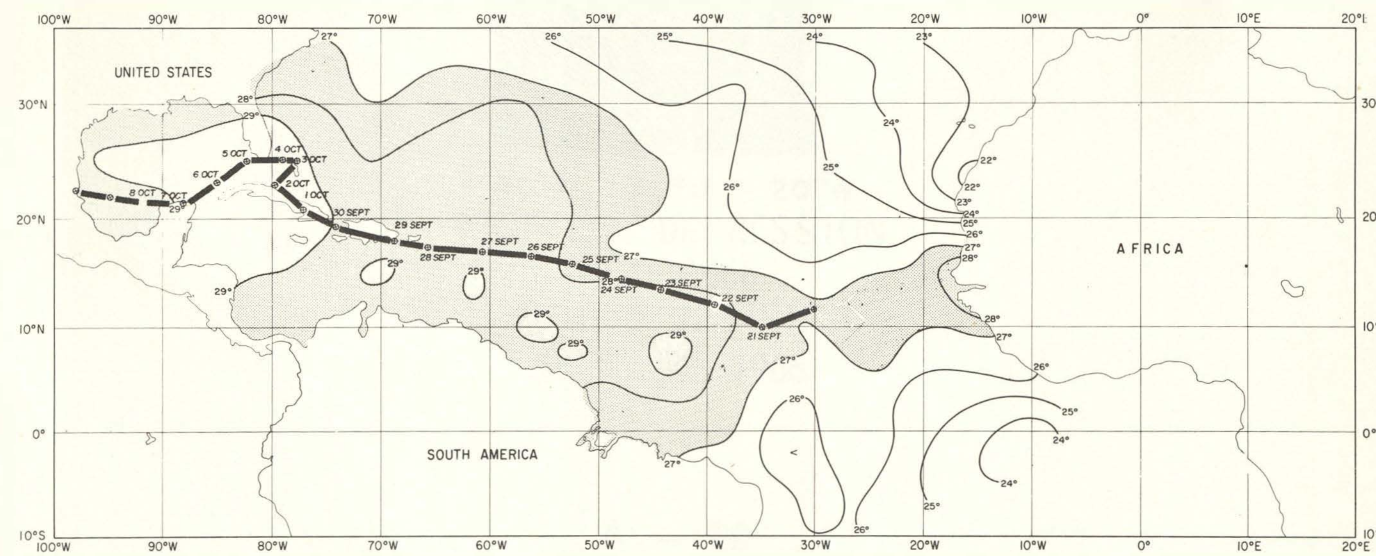

MONTHLY SHIP SEA SURFACE TEMPERATURES (°C)
U. S. NAVY FLEET NUMERICAL WEATHER CENTRAL-MONTERREY, CALIF.)
SEPTEMBER 1966

(b)

TROPICAL DEPRESSION
INEZ 1966
NIMBUS II HRIR
SEPT. 22, 1966

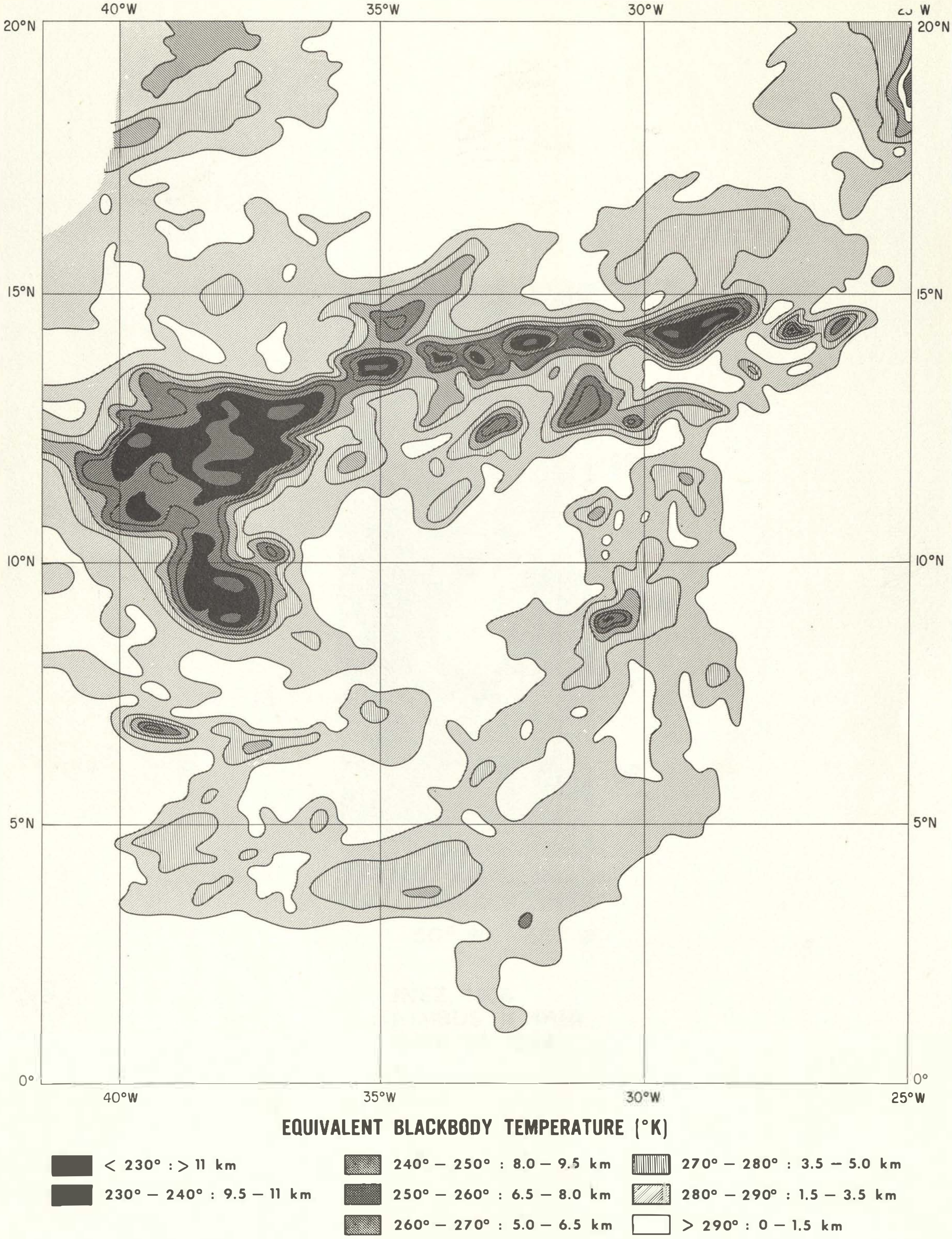

TROPICAL DEPRESSION INEZ, 1966

NIMBUS II HRIR

SEPTEMBER 22, 1966

Figure A-7

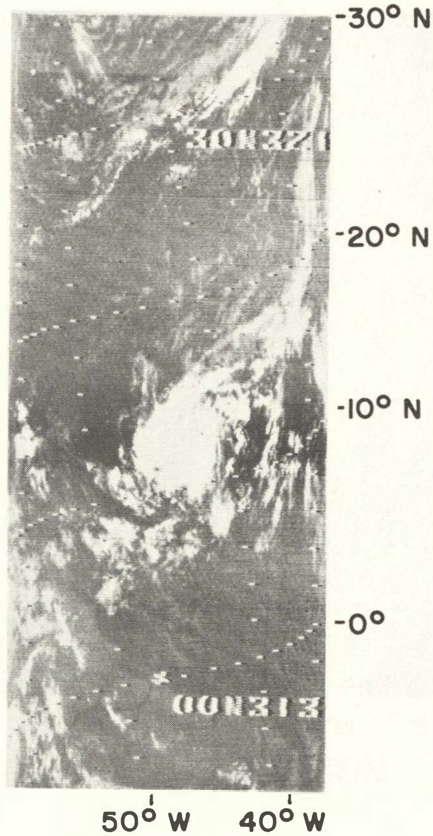

INEZ, 1966
NIMBUS II HRIR
SEPT. 23, 1966

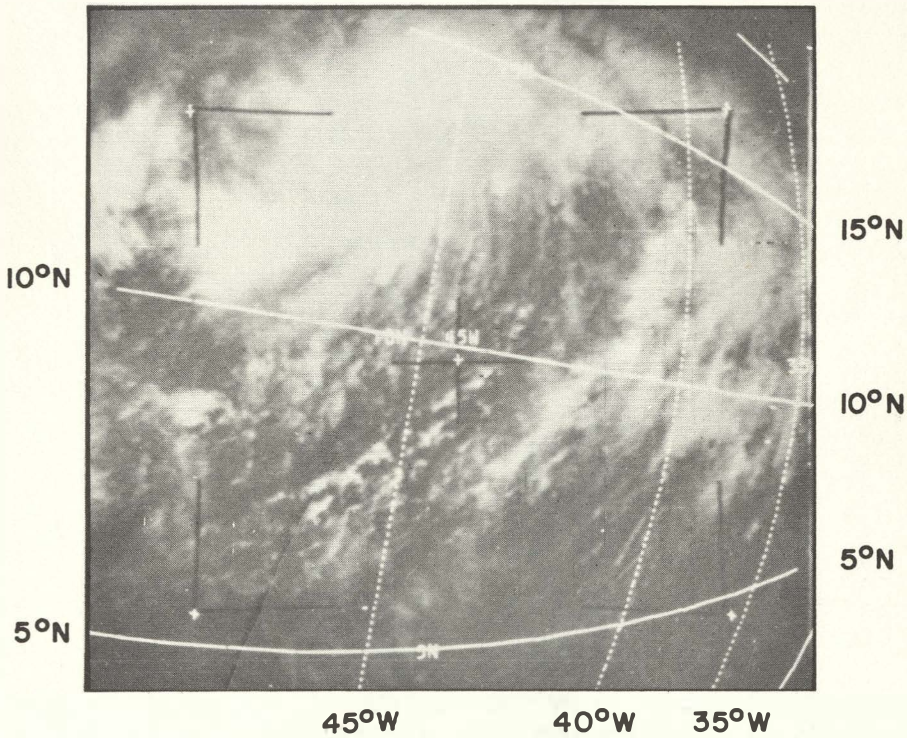

TROPICAL DEPRESSION
INEZ 1966
ESSA I TV
SEPT. 23, 1966

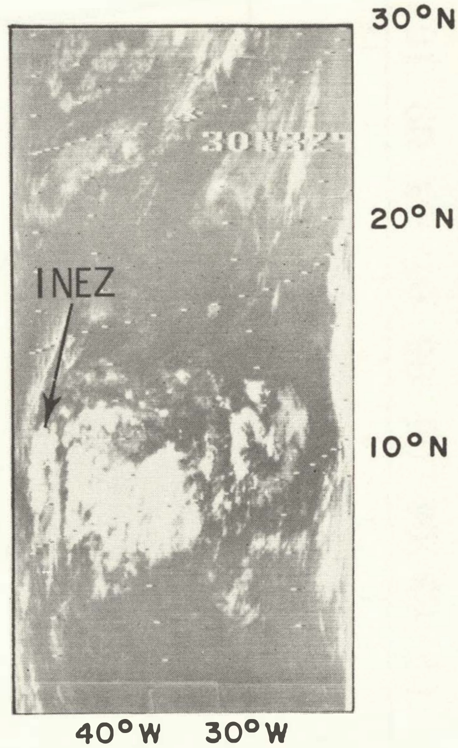

TROPICAL DEPRESSION
INEZ 1966
NIMBUS II HRIR
SEPT. 24, 1966

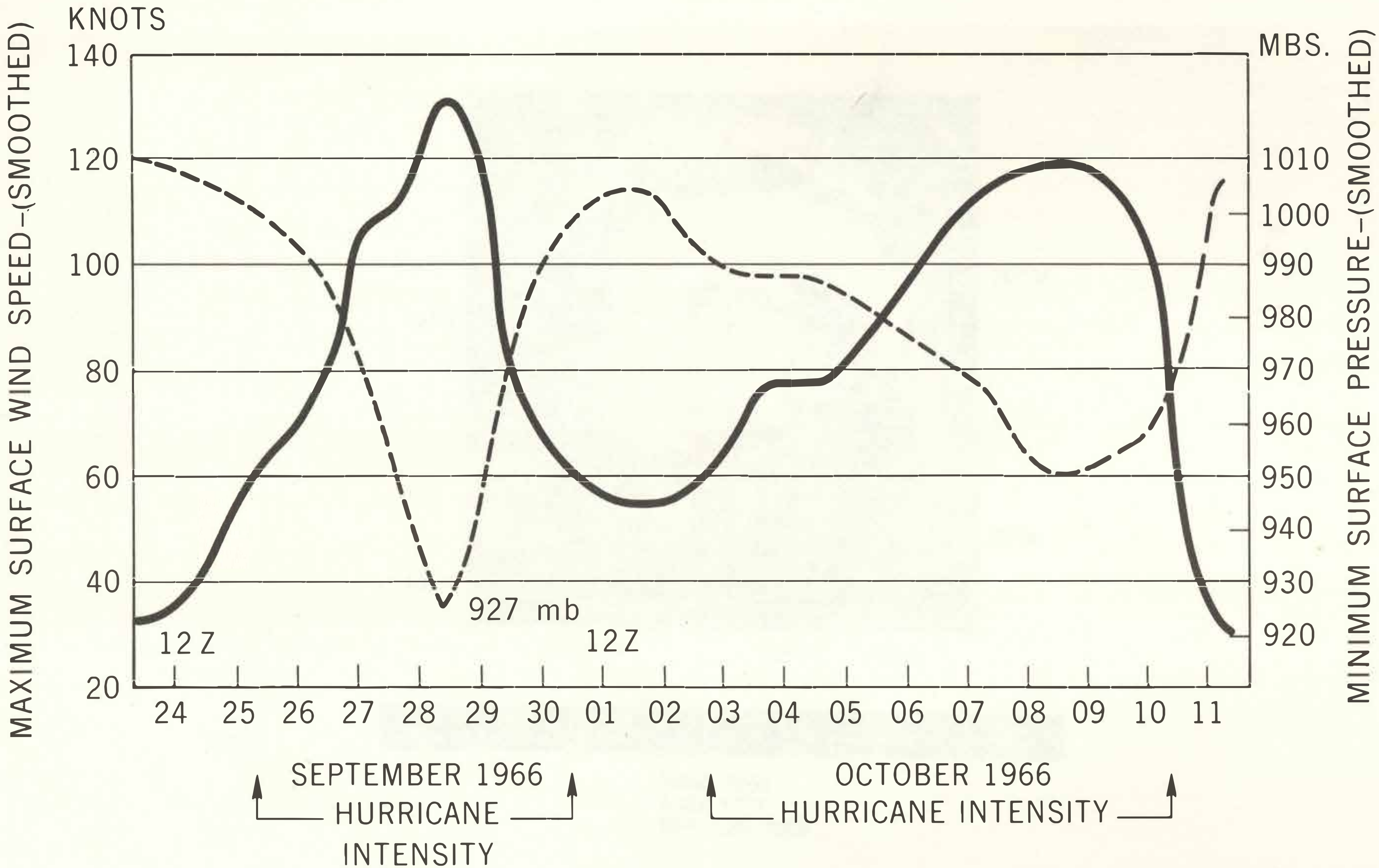

HURRICANE INEZ, 1966

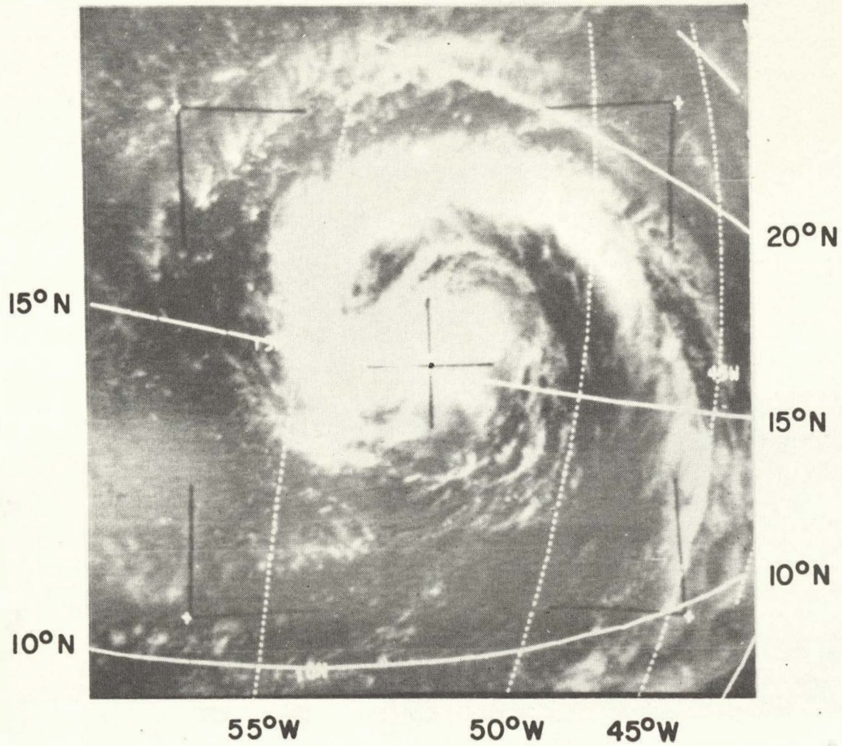

YR	MO	DY	HR	MIN	SC	TK	ZO	S	ESSA	M	C	LAT	SP	LONG	SP	ORBIT	FR	SUN GLINT.
66	9	25	16	52	53	3	55	F	1	T	1	15N	5	55W	5	3363	7	NONE

INEZ, 1966
ESSA I TV
SEPT. 25, 1966

TROPICAL STORM
INEZ 1966
NIMBUS II HRIR
SEPT. 25, 1966

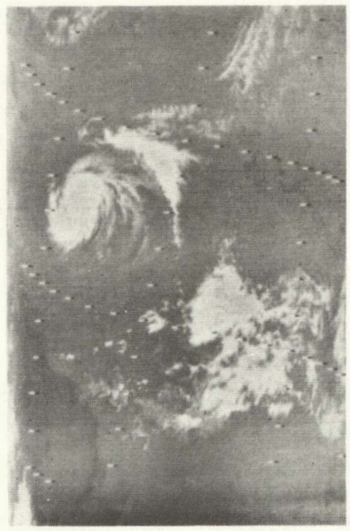

INEZ 1966
NIMBUS II HRIR
SEPT. 26, 1966

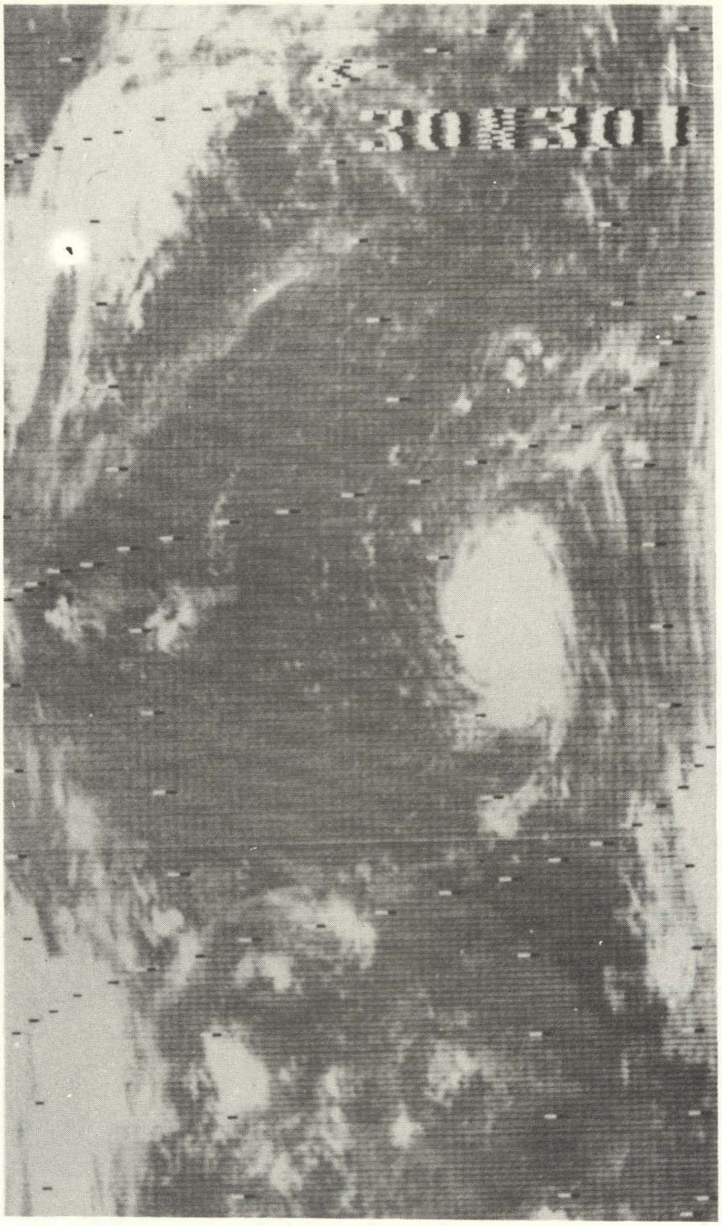

INEZ 1966
NIMBUS II HRIR
SEPT. 27, 1966

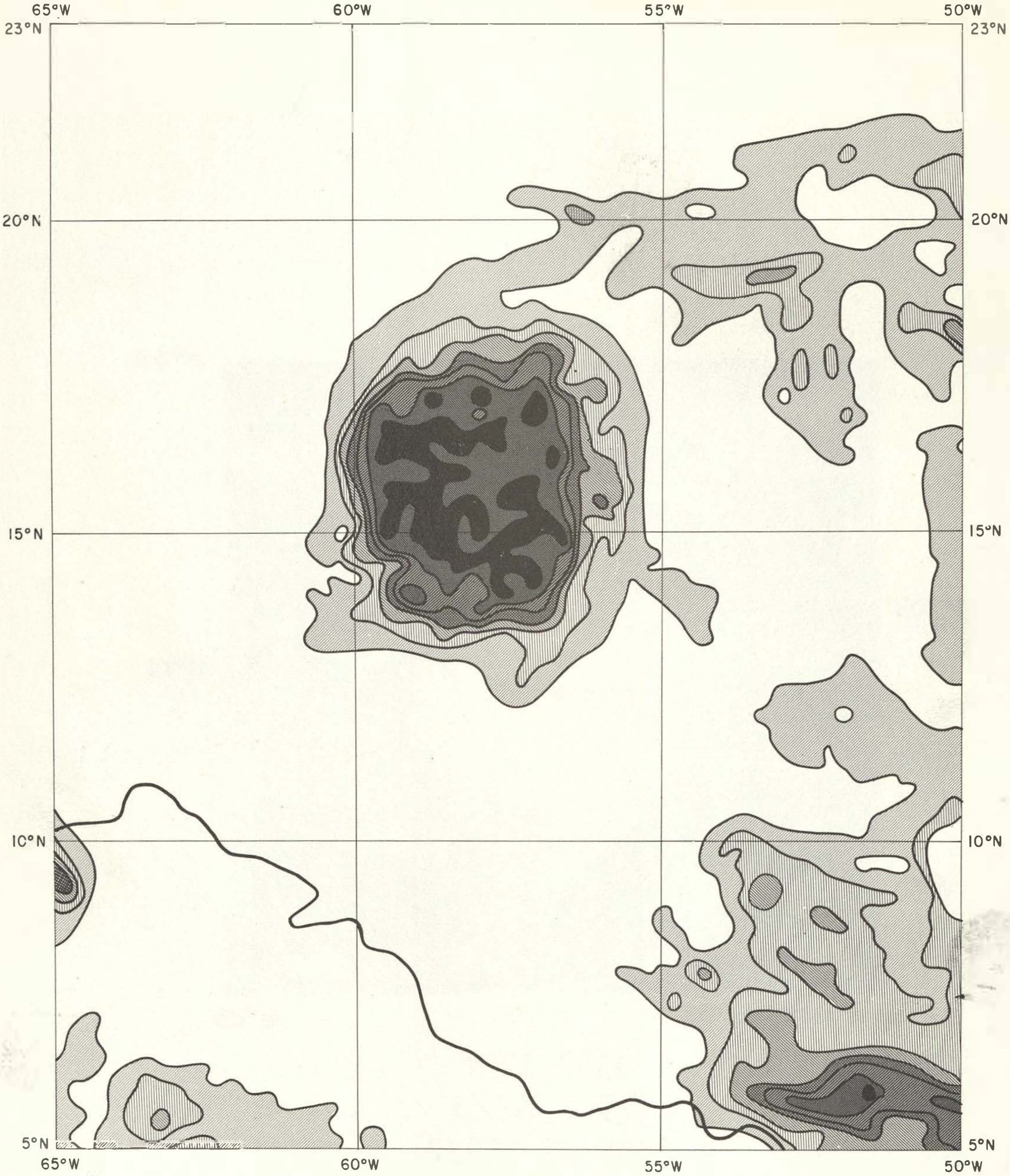

EQUIVALENT BLACKBODY TEMPERATURE (°K)

- < 230° : > 11 km
- 230° – 240° : 9.5 – 11 km
- 240° – 250° : 8.0 – 9.5 km
- 250° – 260° : 6.5 – 8.0 km
- 260° – 270° : 5.0 – 6.5 km
- 270° – 280° : 3.5 – 5.0 km
- 280° – 290° : 1.5 – 3.5 km
- > 290° : 0 – 1.5 km

HURRICANE INEZ, 1966

NIMBUS II HRIR

SEPTEMBER 27, 1966

Figure A-26

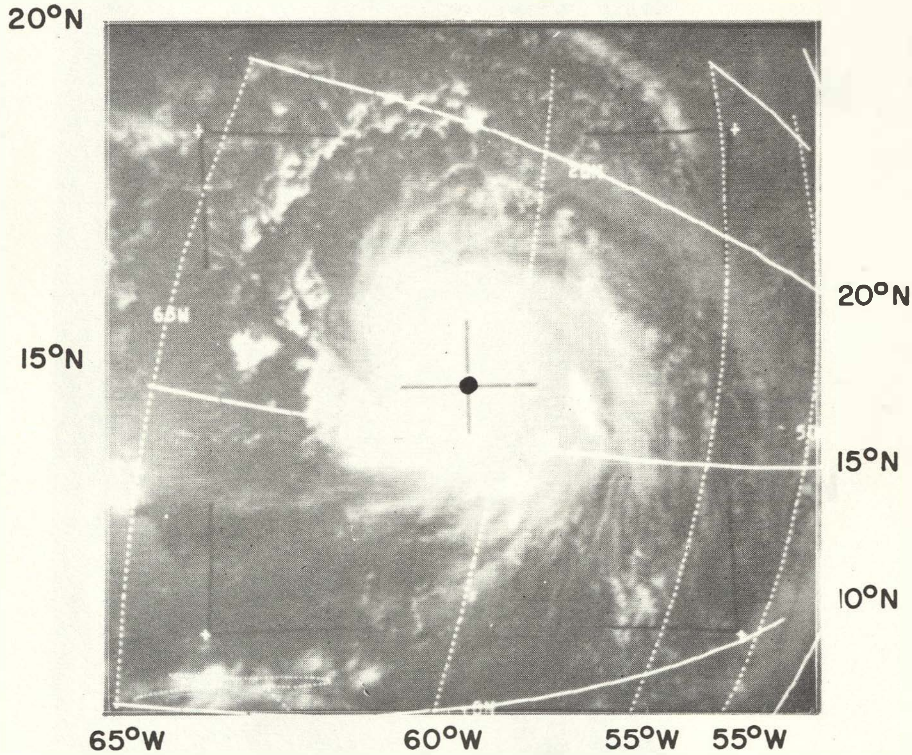

INEZ 1966
ESSA I TV
SEPT. 27, 1966

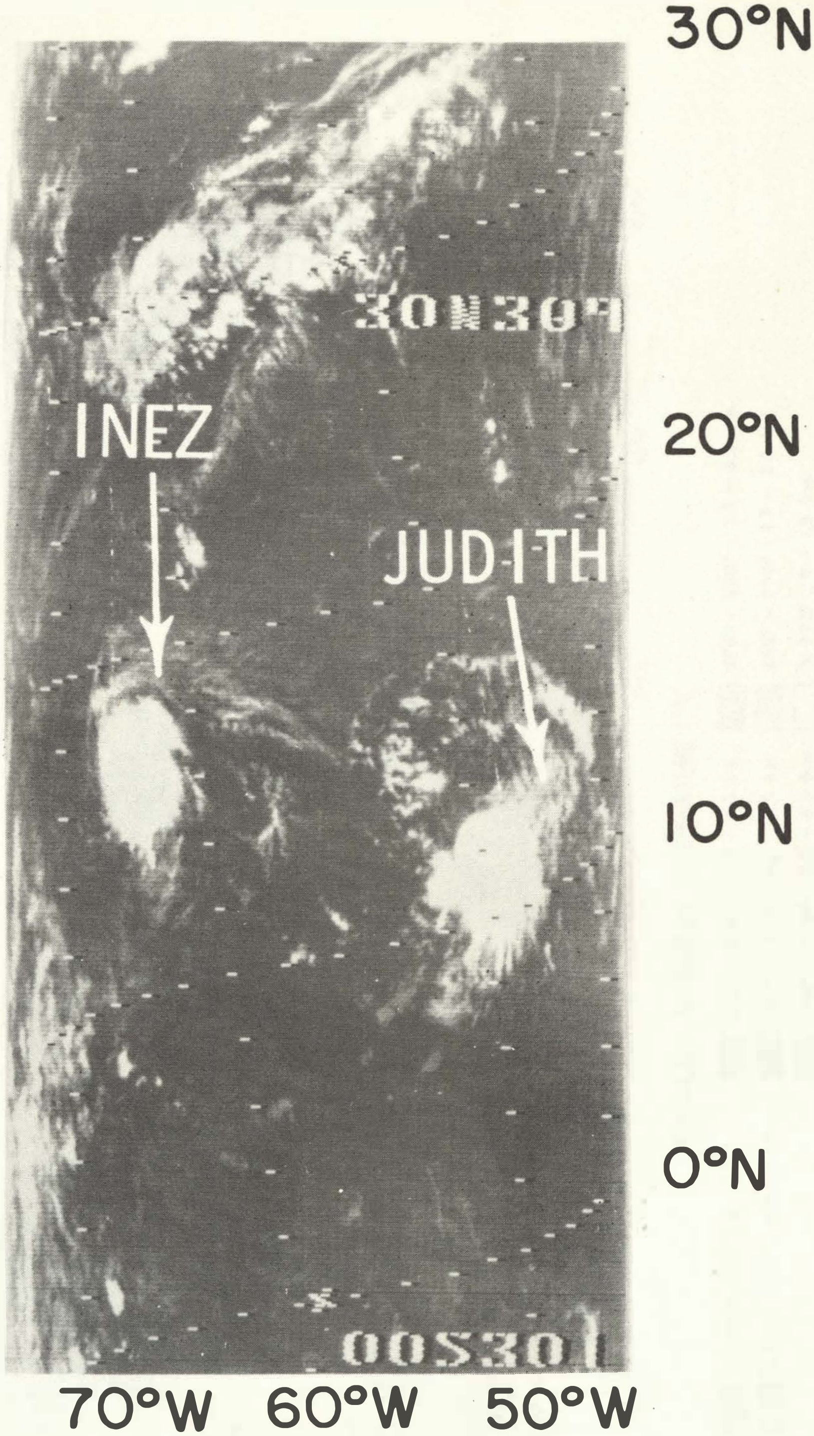

INEZ 1966 AND JUDITH
NIMBUS II HRIR
SEPT. 28, 1966

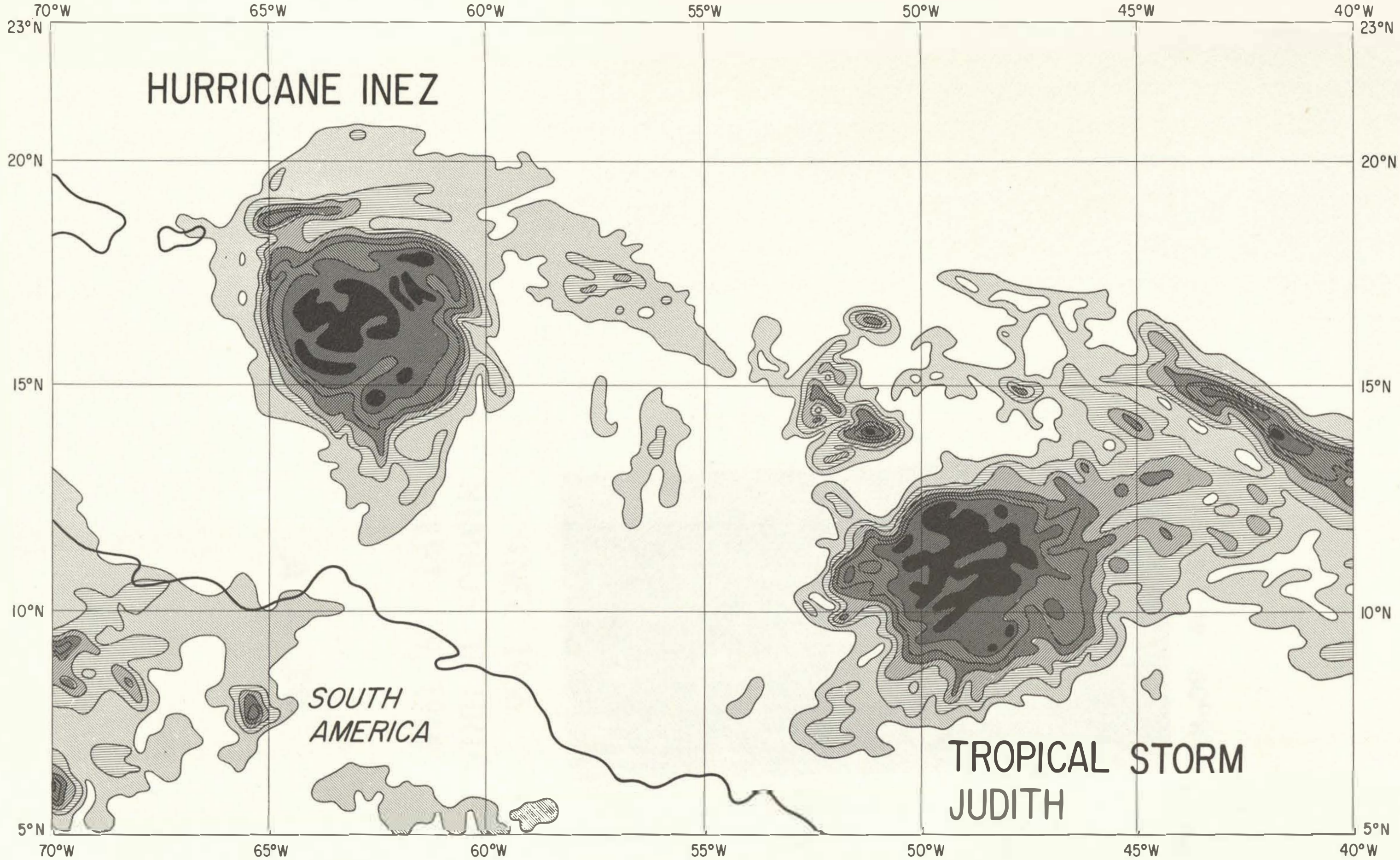

EQUIVALENT BLACKBODY TEMPERATURE (°K)

- < 230° : > 11 km
- 230° – 240° : 9.5 – 11 km
- 240° – 250° : 8.0 – 9.5 km
- 250° – 260° : 6.5 – 8.0 km
- 260° – 270° : 5.0 – 6.5 km
- 270° – 280° : 3.5 – 5.0 km
- 280° – 290° : 1.5 – 3.5 km
- > 290° : 0 – 1.5 km

INEZ AND JUDITH, 1966

NIMBUS II HRIR

SEPTEMBER 28, 1966

Figure A-29

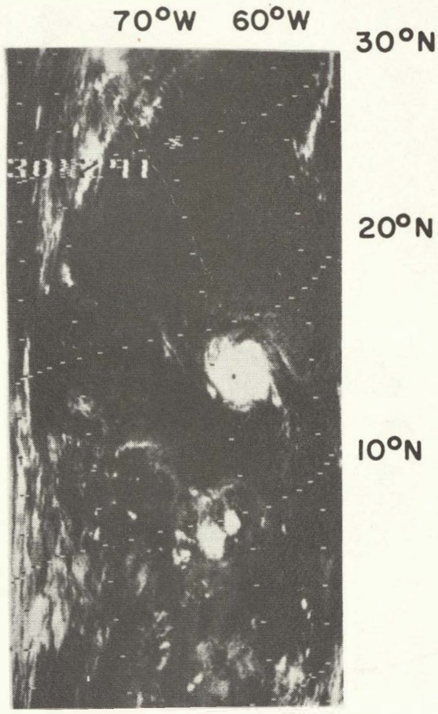

INEZ 1966
NIMBUS II HRIR
SEPT. 29, 1966

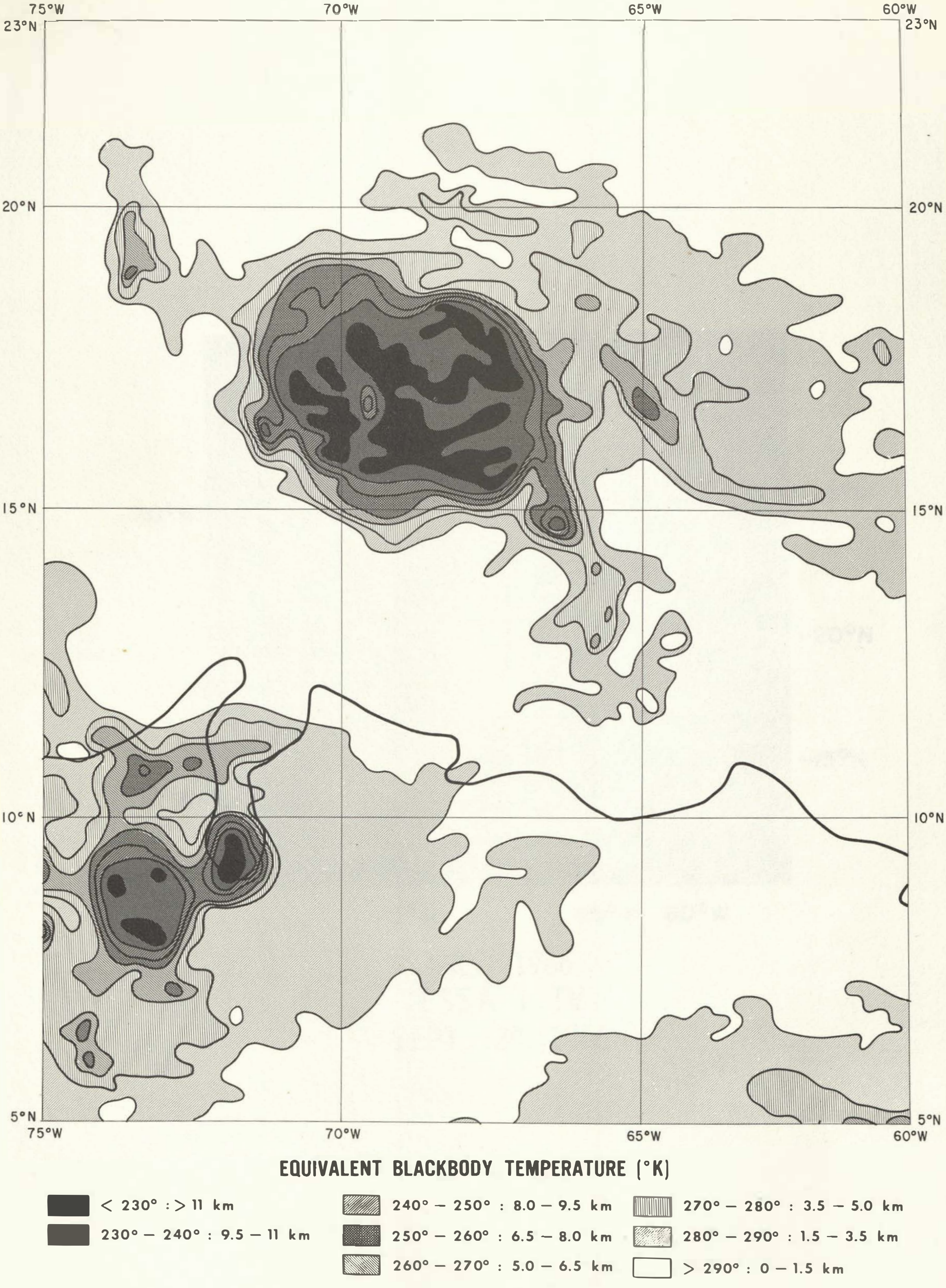

HURRICANE INEZ, 1966

NIMBUS II HRIR

SEPTEMBER 29, 1966

Figure A-31

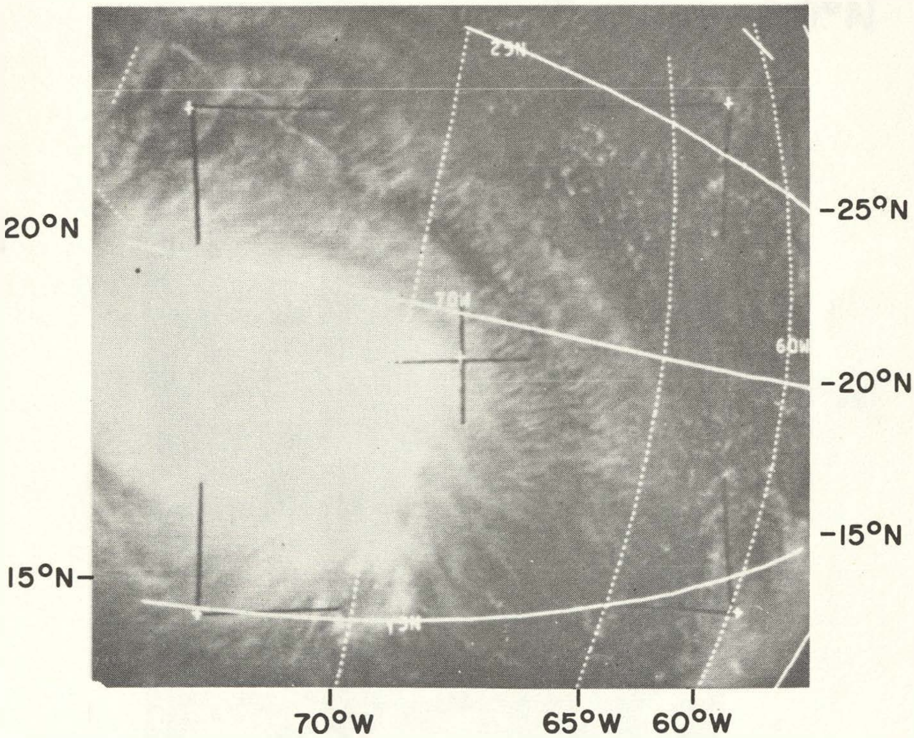

INEZ 1966
ESSA I TV
SEPT. 29, 1966

INEZ 1966 AND TROPICAL STORM JUDITH 1966 NIMBUS II HRIR SEPT. 30, 1966

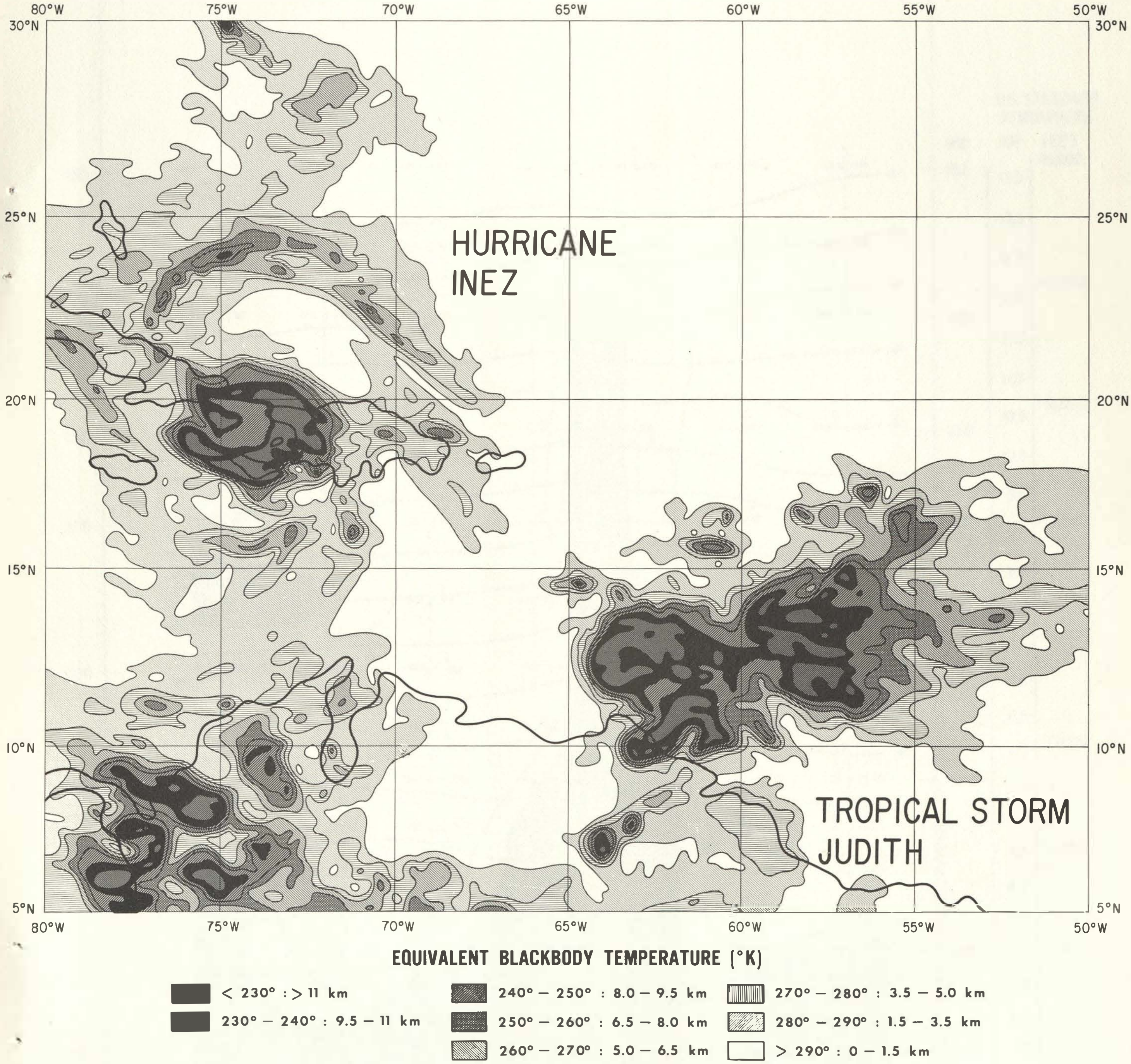

HURRICANE INEZ AND TROPICAL STORM JUDITH

NIMBUS II HRIR

SEPTEMBER 30, 1966

Figure A-34

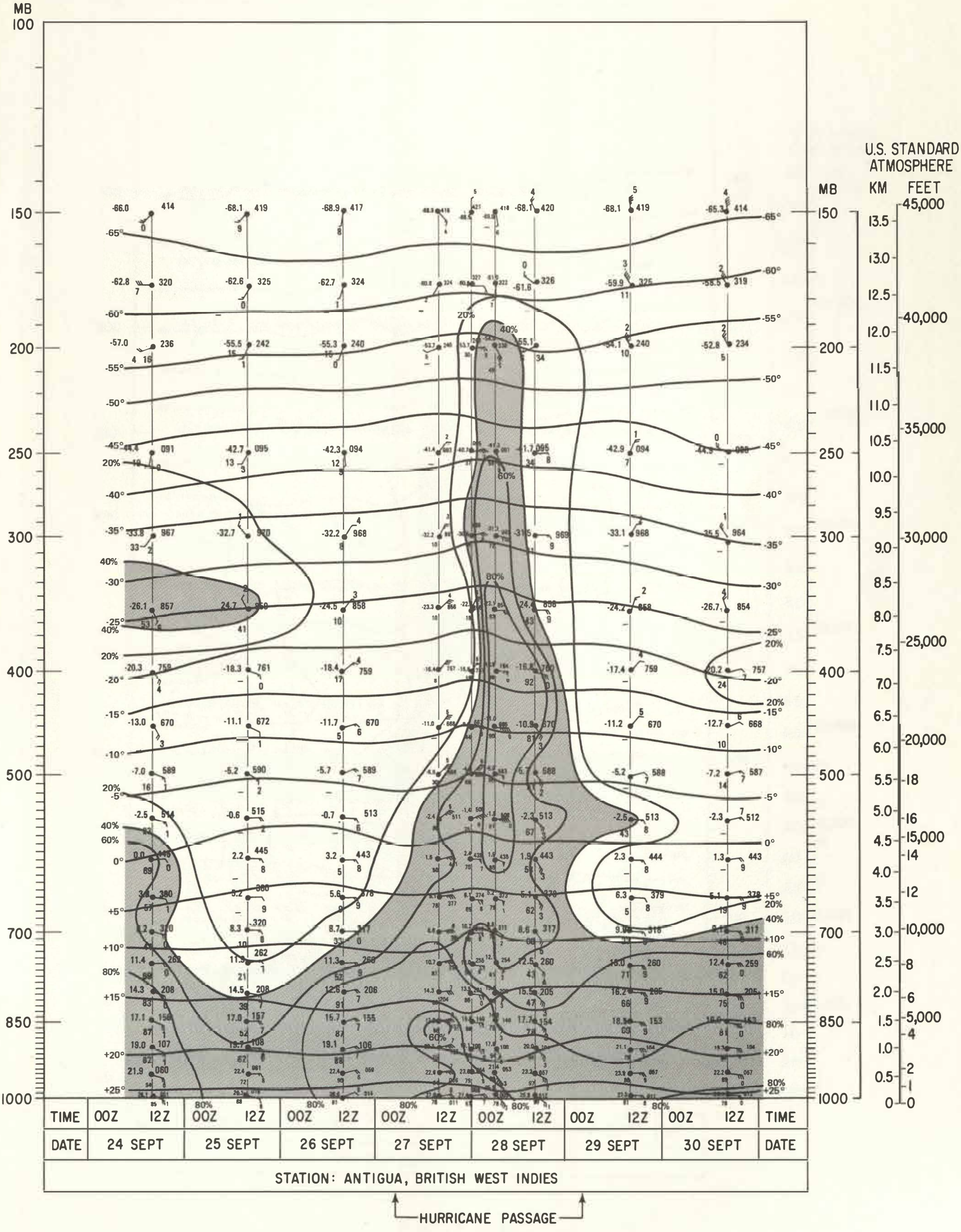
MB
100
150
200
250
300
400
500
700
850
1000
U.S. STANDARD ATMOSPHERE
MB
KM
FEET
45,000
40,000
35,000
30,000
25,000
20,000
15,000
10,000
5,000
TIME
00Z
12Z
DATE
24 SEPT
25 SEPT
26 SEPT
27 SEPT
28 SEPT
29 SEPT
30 SEPT
STATION: ANTIGUA, BRITISH WEST INDIES
HURRICANE PASSAGE

Figure A-35

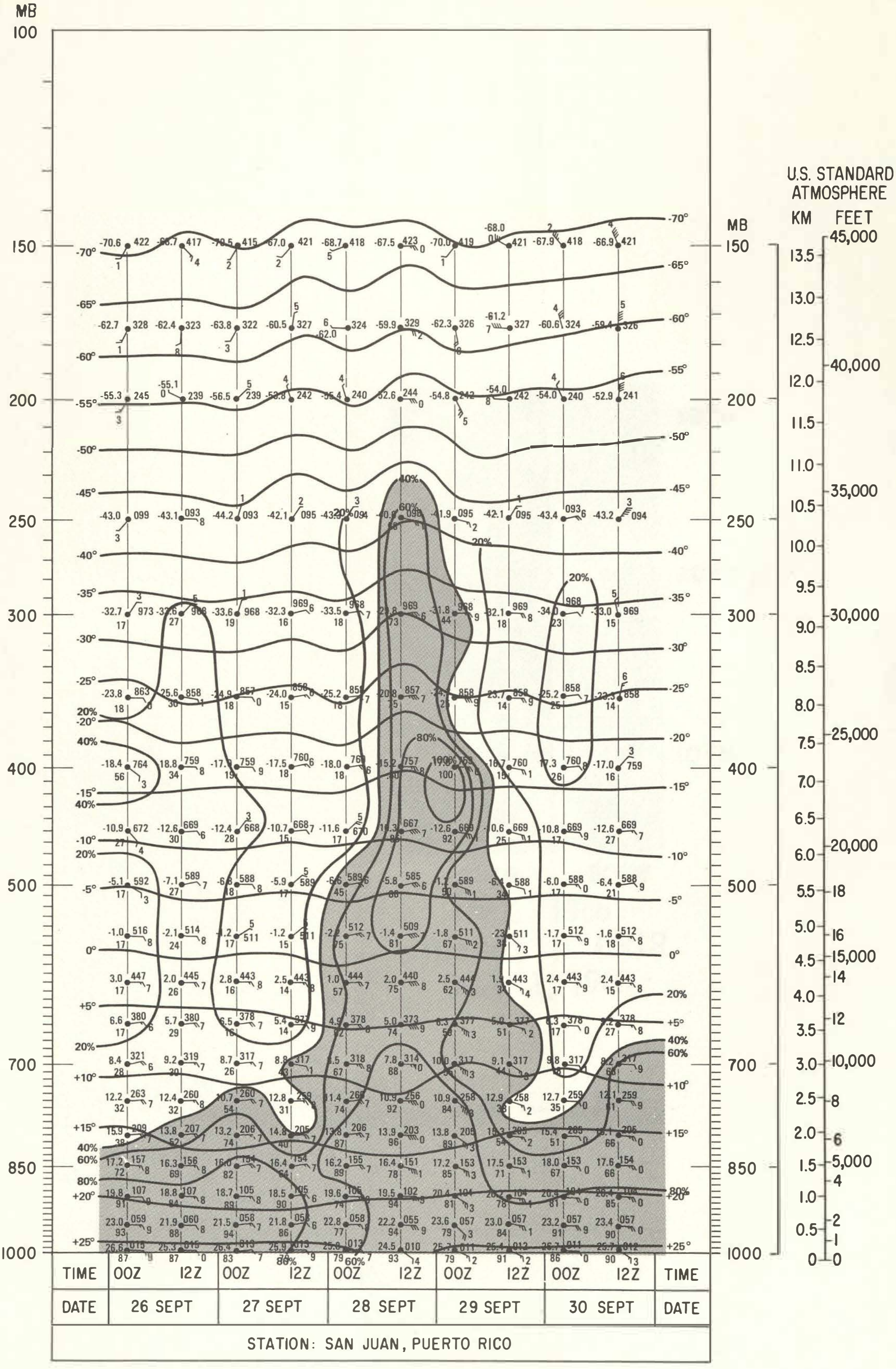
MB
U.S. STANDARD ATMOSPHERE
KM
FEET
TIME
00Z
12Z
DATE
26 SEPT
27 SEPT
28 SEPT
29 SEPT
30 SEPT
STATION: SAN JUAN, PUERTO RICO

Figure A-36

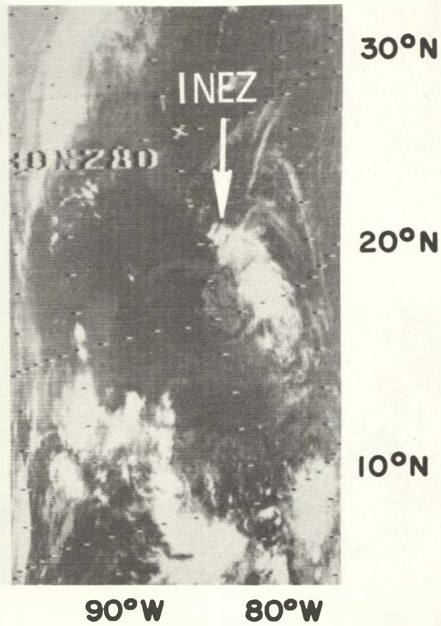

INEZ 1966
NIMBUS II HRIR
OCT. 1, 1966

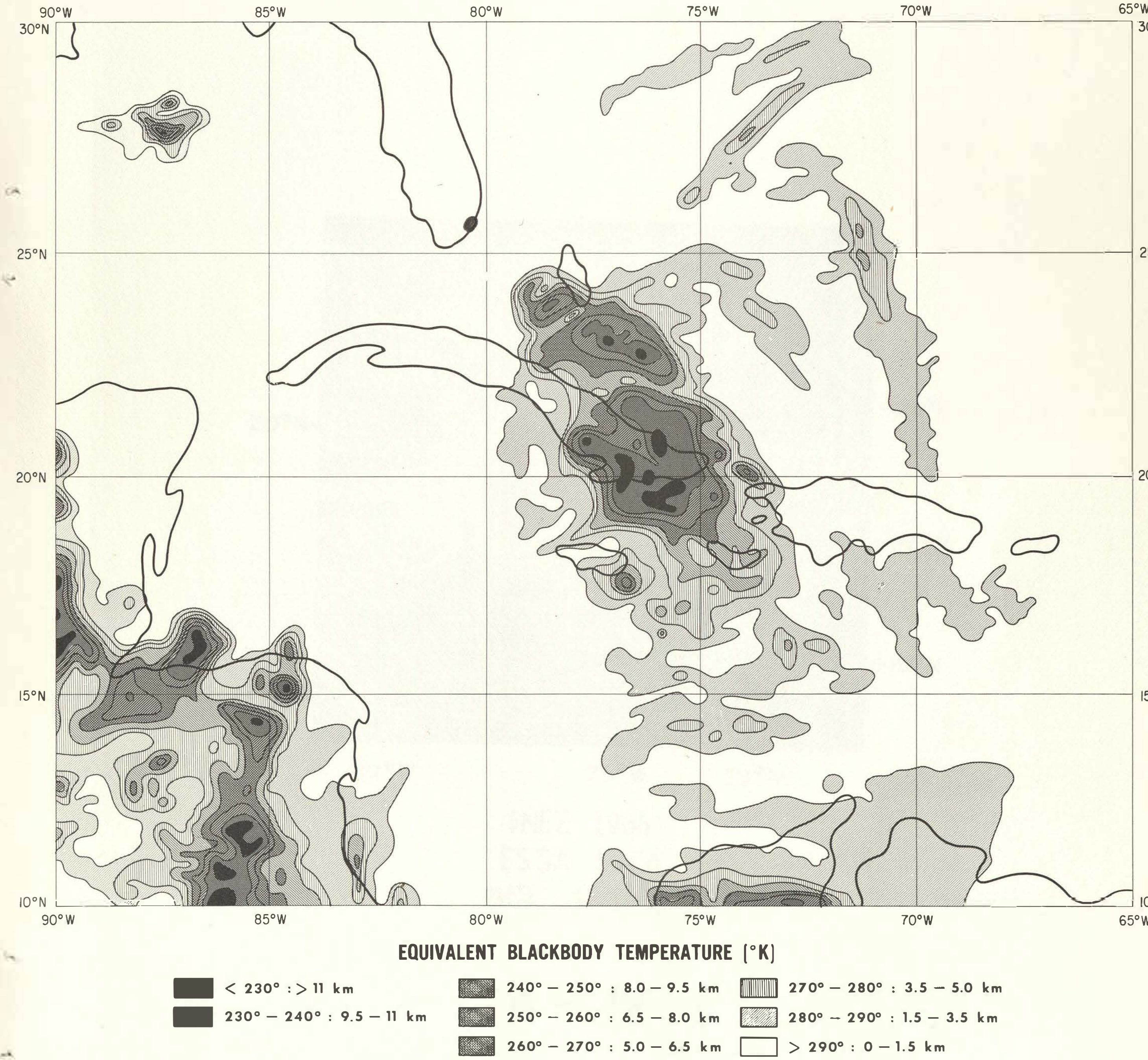

TROPICAL STORM INEZ, 1966

NIMBUS II HRIR

OCTOBER 1, 1966

Figure A-38

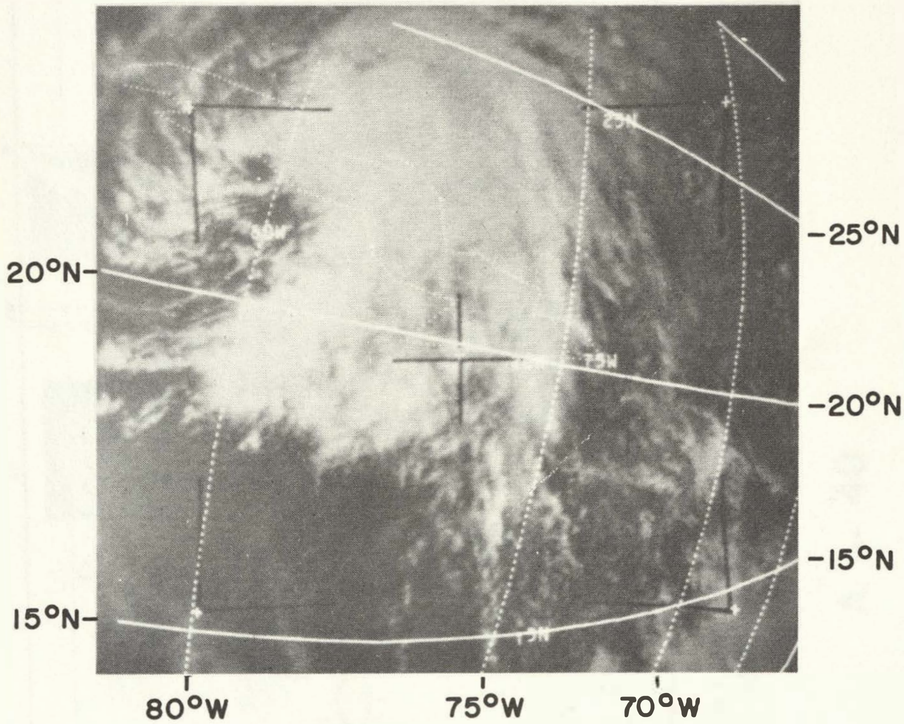

INEZ 1966
ESSA I TV
OCT. 1, 1966

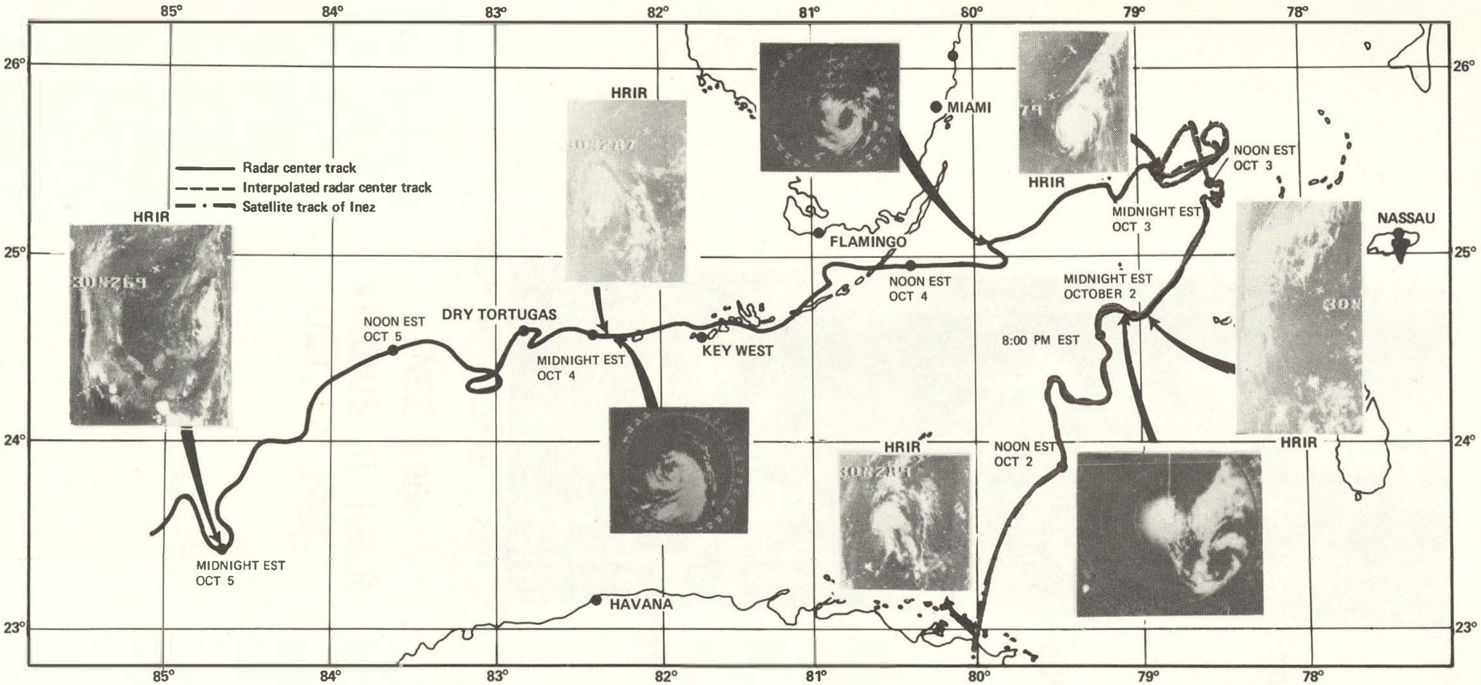

KEY WEST – MIAMI COMBINED RADAR TRACK AND NIMBUS II HRIR DATA
OF HURRICANE INEZ OCTOBER 2–6, 1966

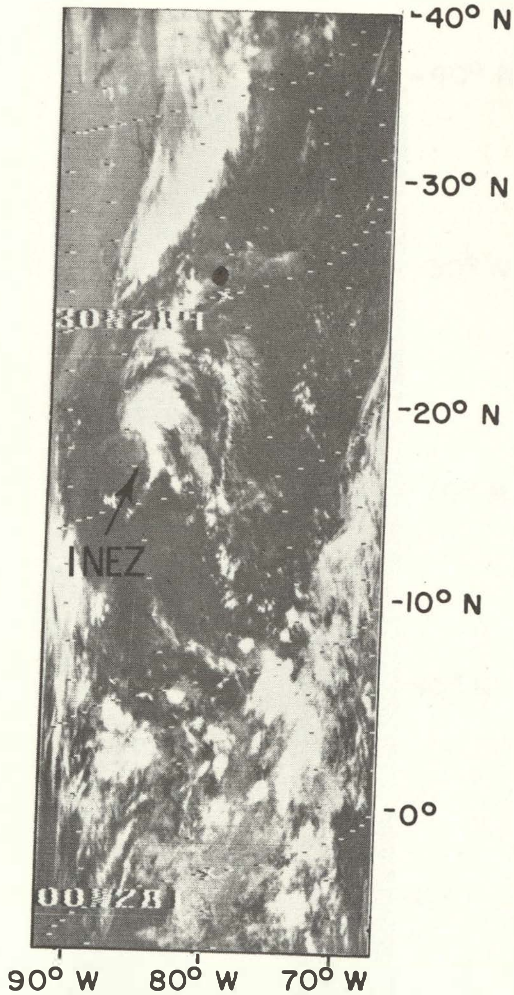

INEZ 1966
NIMBUS II HRIR
OCT. 2, 1966

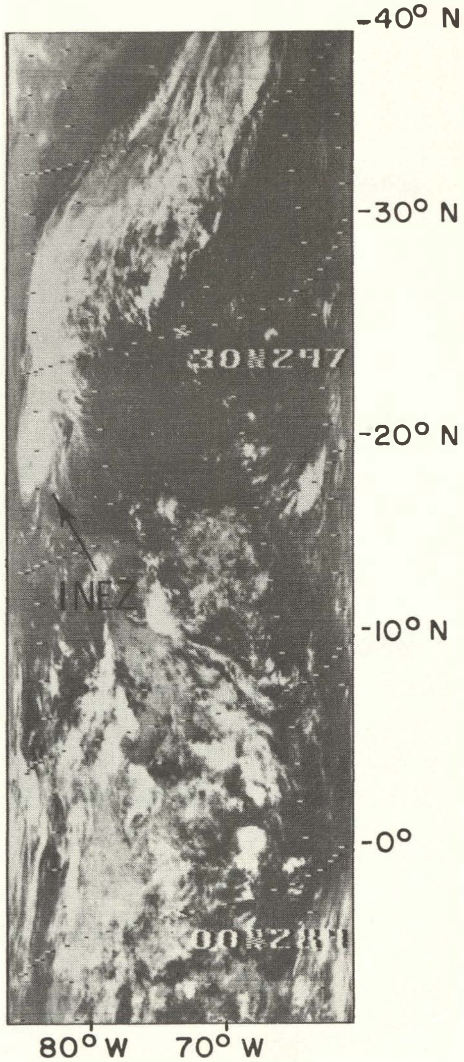

INEZ 1966
NIMBUS II HRIR
OCT. 3, 1966

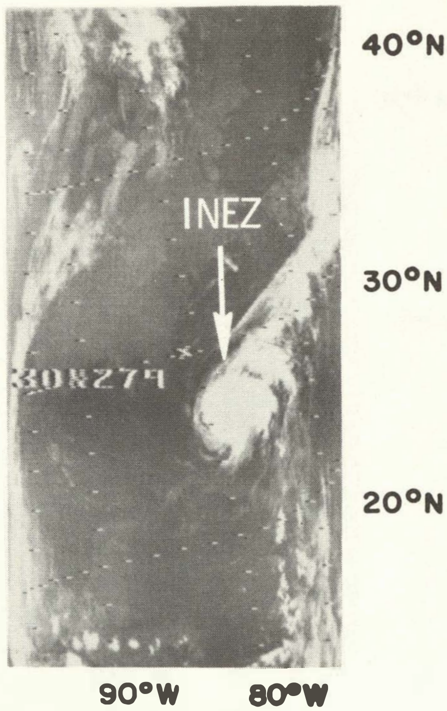

INEZ 1966
NIMBUS II HRIR
OCT. 4, 1966

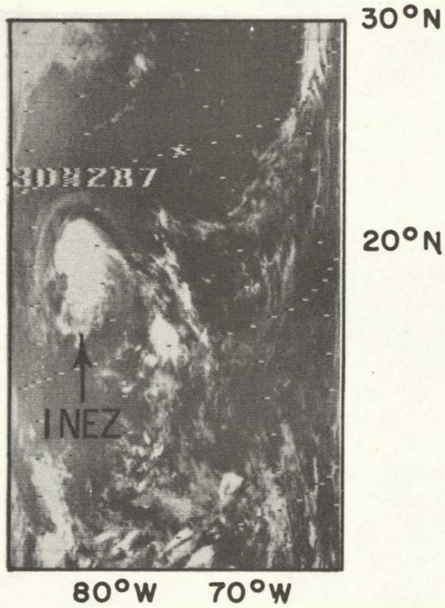

INEZ 1966
NIMBUS II HRIR
OCT. 5, 1966

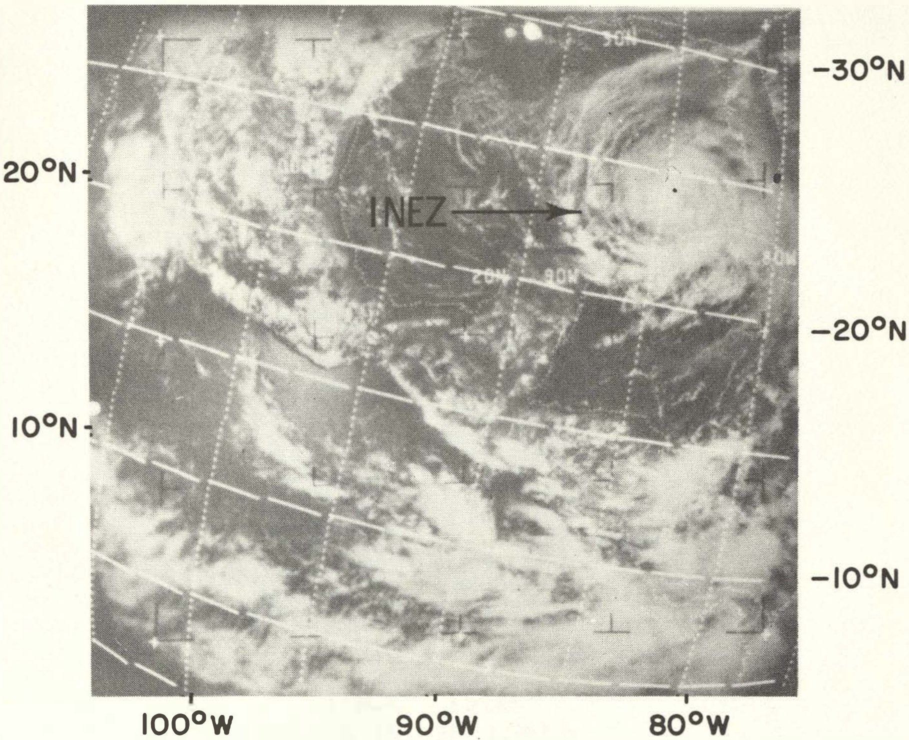

INEZ 1966
ESSA III TV
OCT. 5, 1966

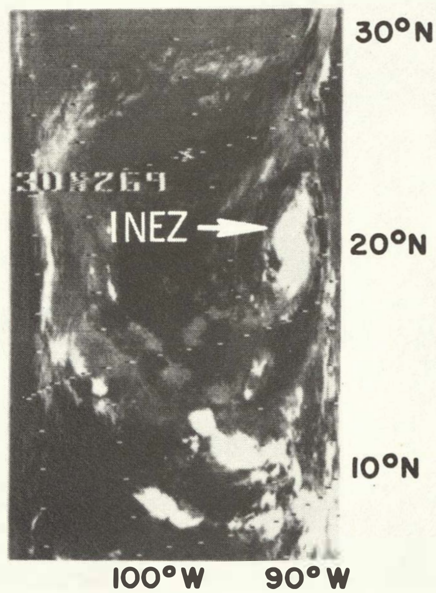

INEZ 1966
NIMBUS II HRIR
OCT. 6, 1966

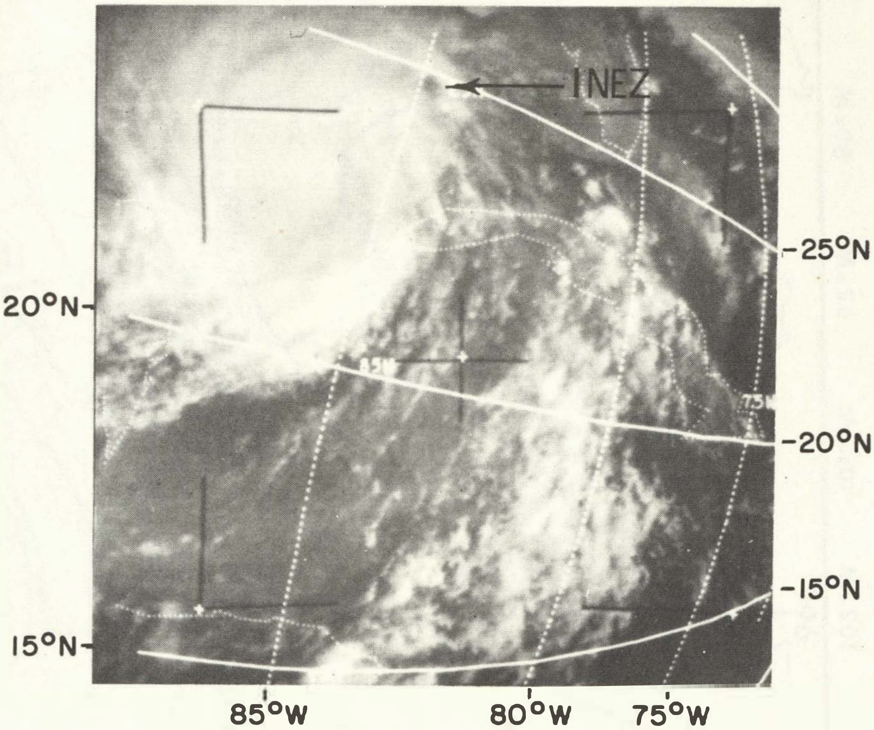

INEZ 1966
ESSA I TV
OCT. 6, 1966

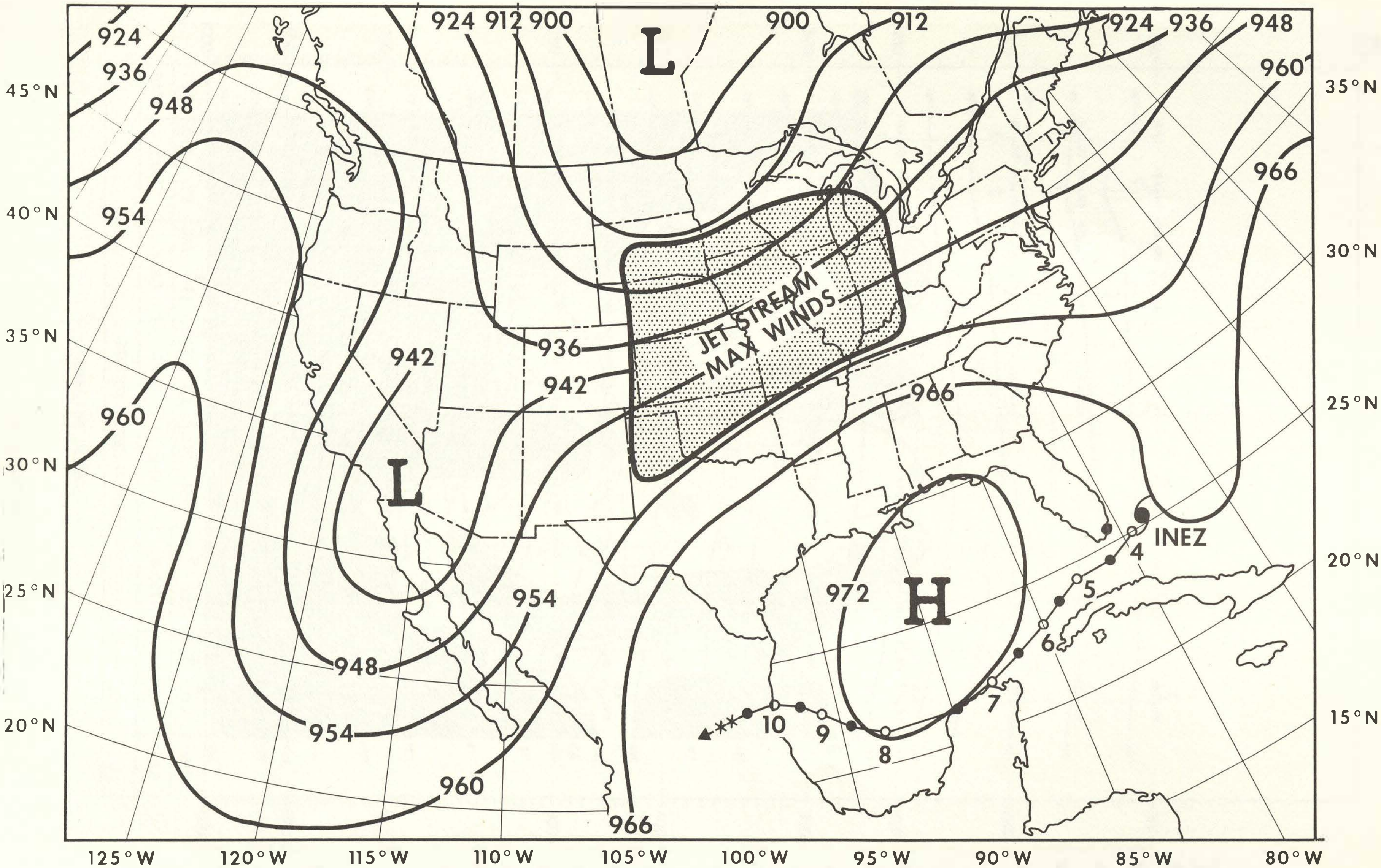

······ TROPICAL DEPRESSION (DEVELOPMENT) STAGE
– – – TROPICAL STORM STAGE
——— HURRICANE STAGE
✱✱✱ DEPRESSION (DISSIPATION) STAGE
○ POSITION AT 7:00 A.M. E.S.T.
● POSITION AT 7:00 P.M. E.S.T.

300 MB CHART 00 GMT OCTOBER 4, 1966

Figure A-48

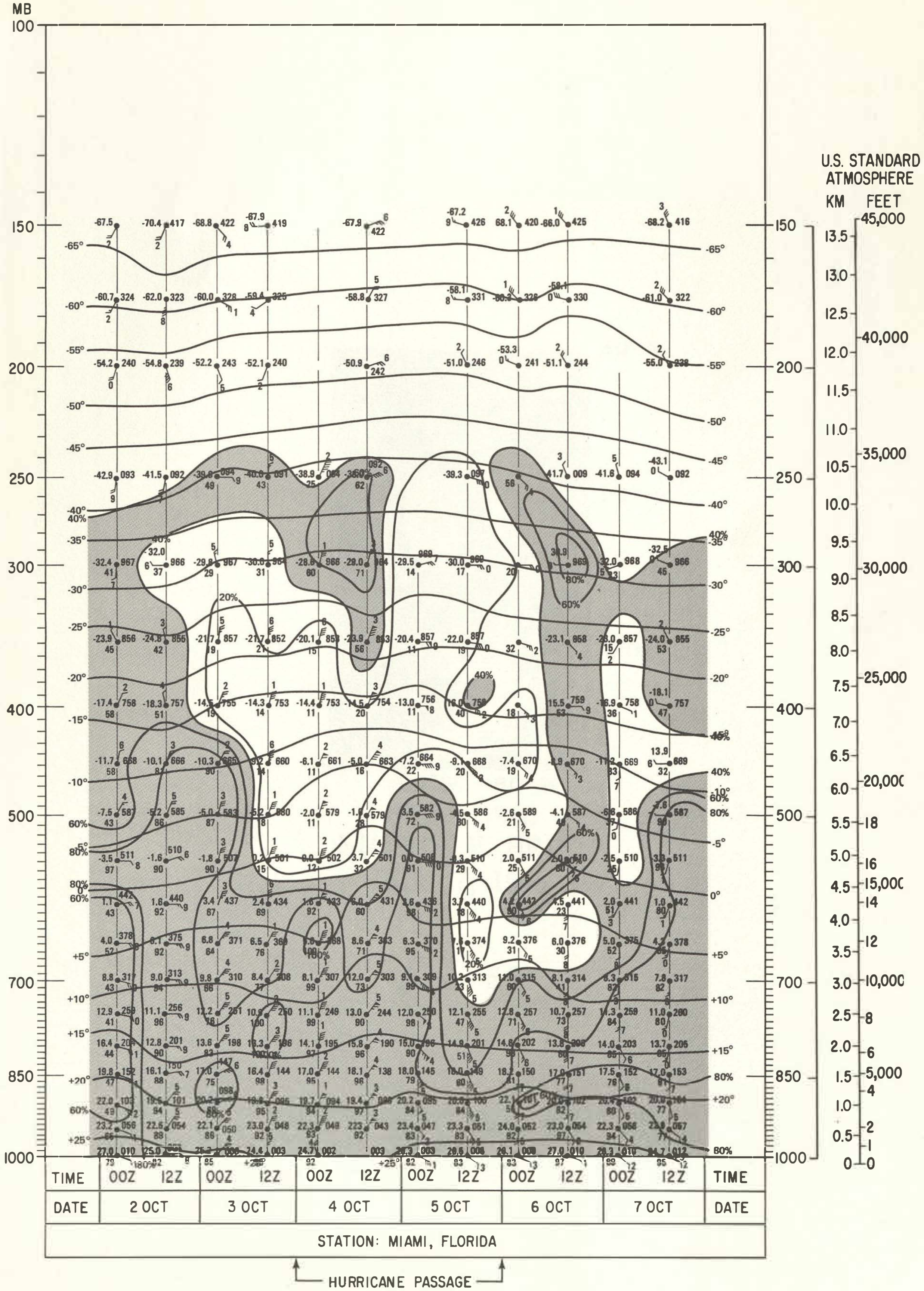

MB
U.S. STANDARD ATMOSPHERE
KM
FEET
TIME
DATE
2 OCT
3 OCT
4 OCT
5 OCT
6 OCT
7 OCT
STATION: MIAMI, FLORIDA
HURRICANE PASSAGE

Figure A-49

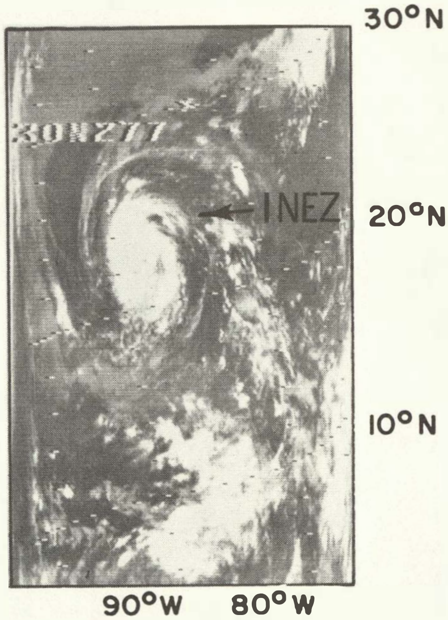

INEZ 1966
NIMBUS II HRIR
OCT. 7, 1966

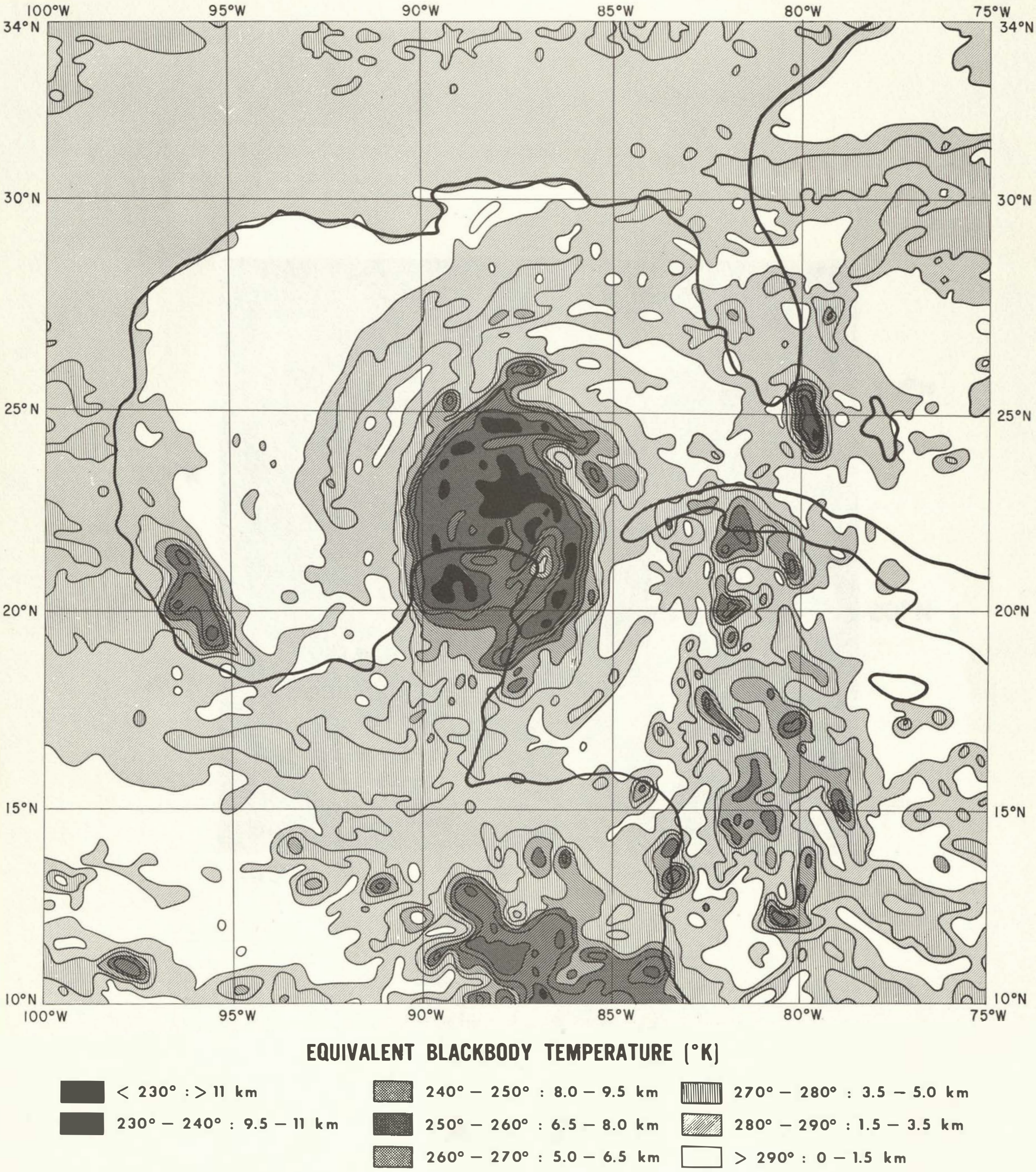

HURRICANE INEZ, 1966

NIMBUS II HRIR

OCTOBER 7, 1966

Figure A-51

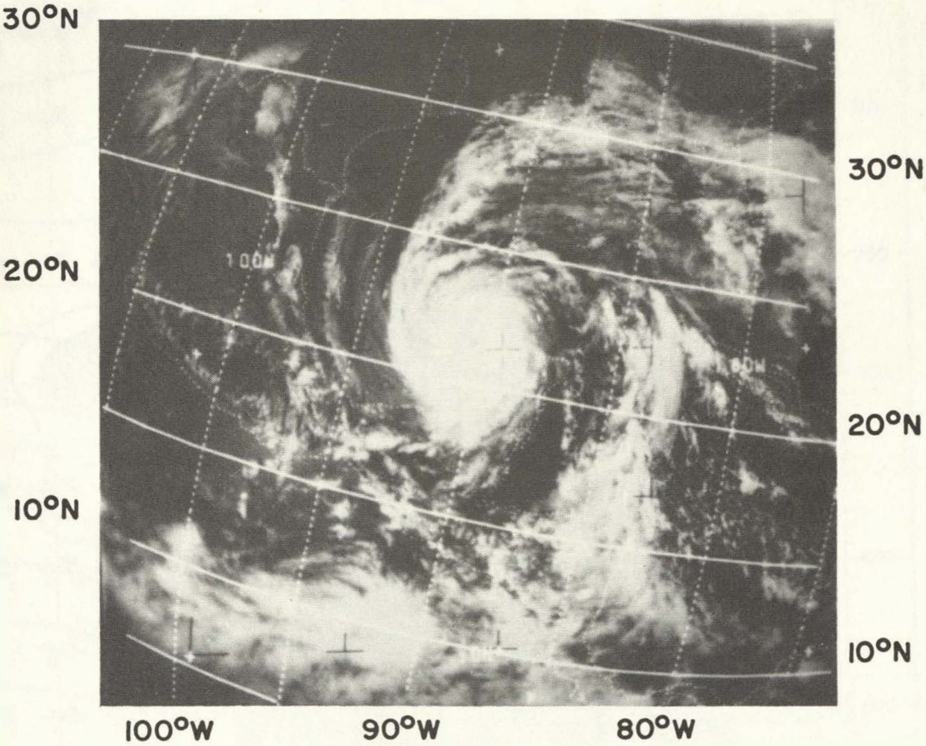

INEZ 1966
ESSA III TV
OCT. 7, 1966

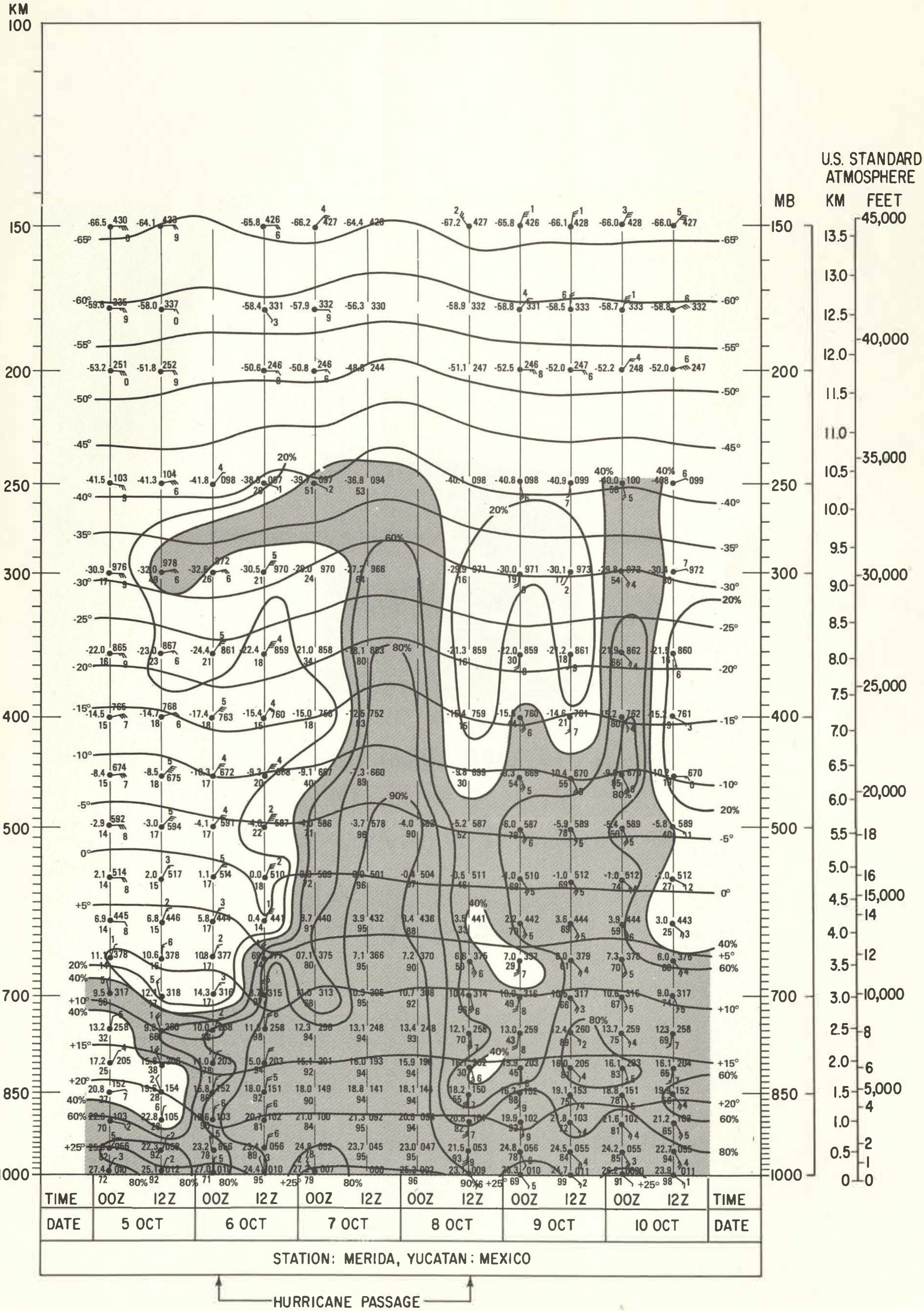

KM
100
U.S. STANDARD ATMOSPHERE
MB
KM
FEET
TIME
DATE
00Z
12Z
5 OCT
6 OCT
7 OCT
8 OCT
9 OCT
10 OCT
STATION: MERIDA, YUCATAN: MEXICO
HURRICANE PASSAGE

Figure A-53

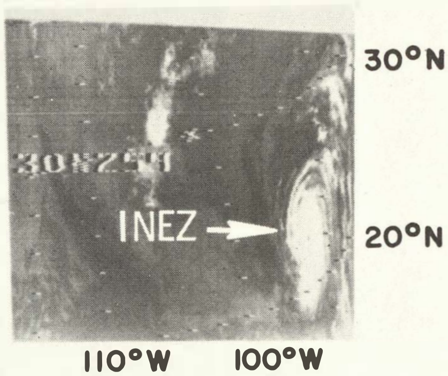

INEZ 1966
NIMBUS II HRIR
OCT. 8, 1966

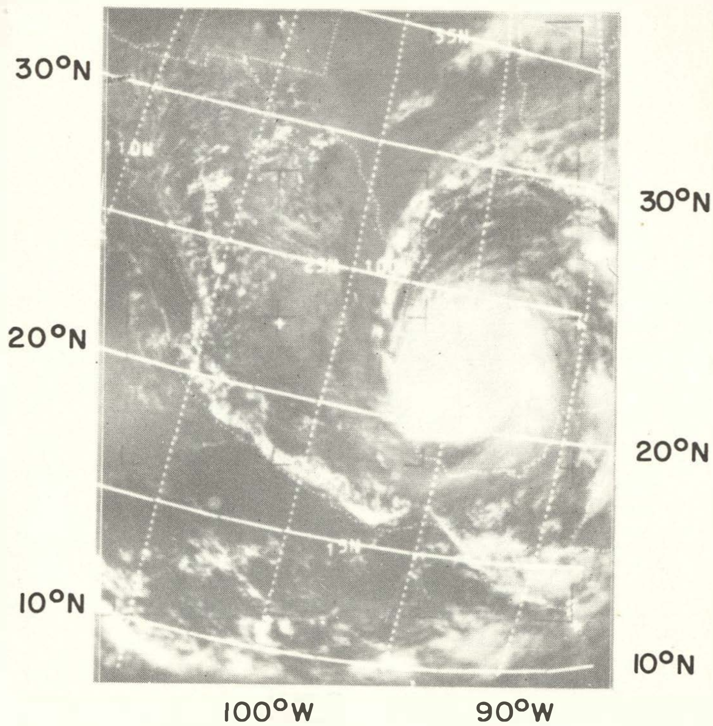

INEZ 1966
ESSA III TV
OCT. 8, 1966

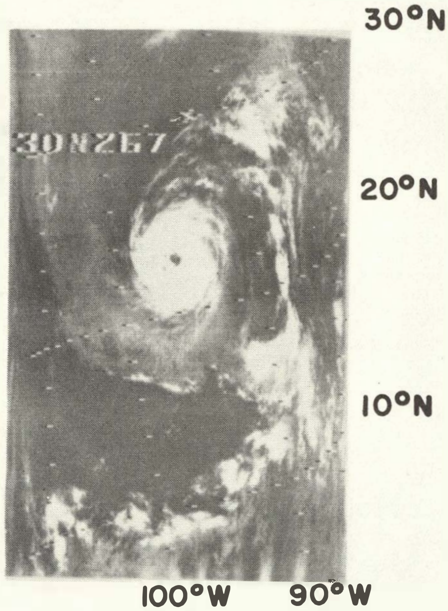

INEZ 1966
NIMBUS II HRIR
OCT. 9, 1966

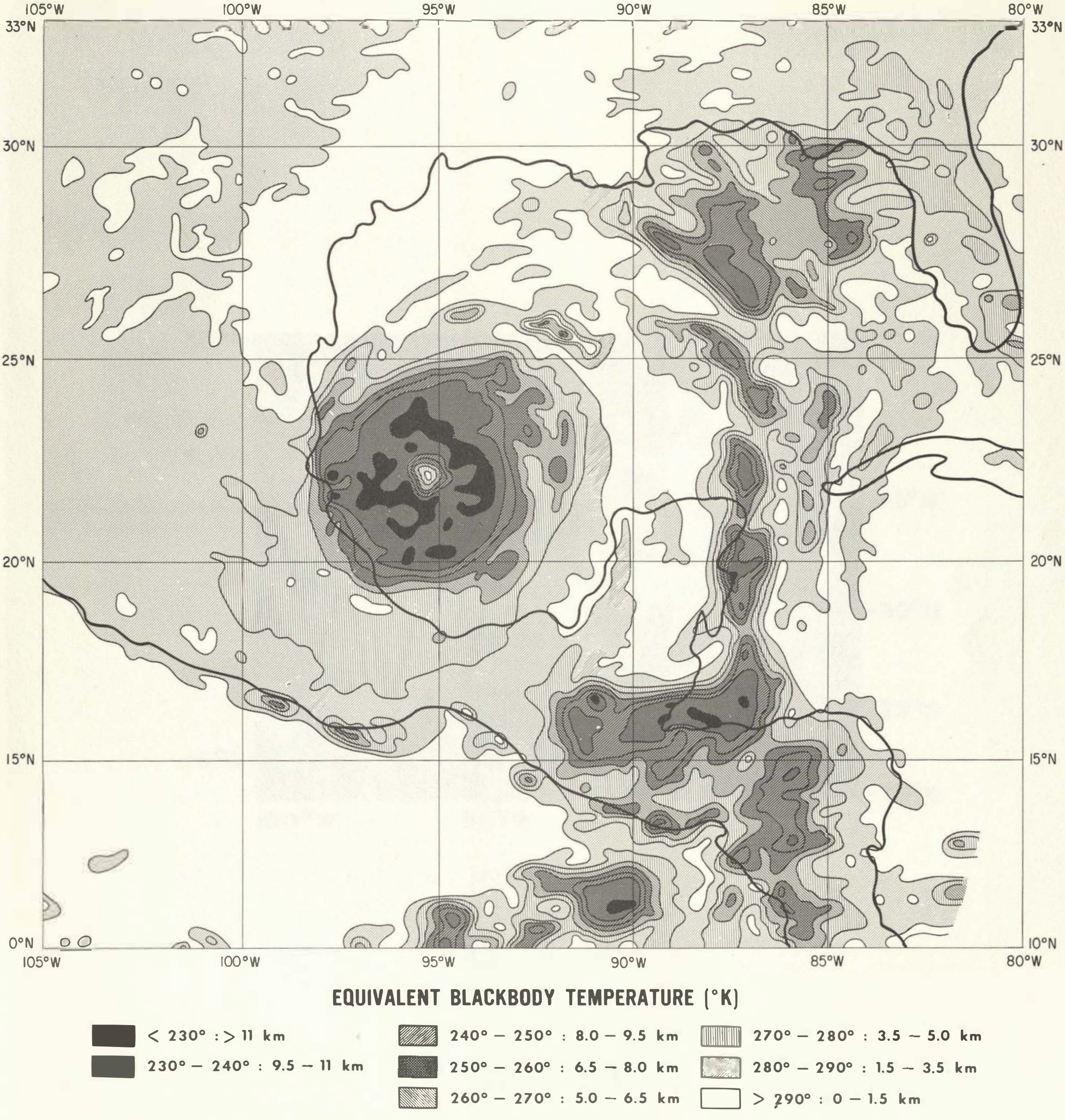

HURRICANE INEZ, 1966

NIMBUS II HRIR

OCTOBER 9, 1966

Figure A-57

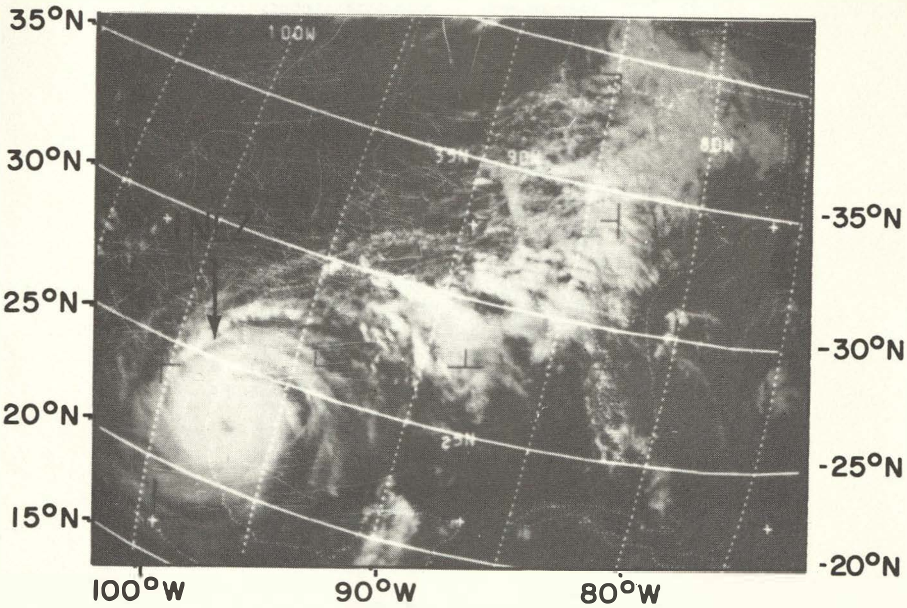

INEZ 1966
ESSA III TV
OCT. 9, 1966

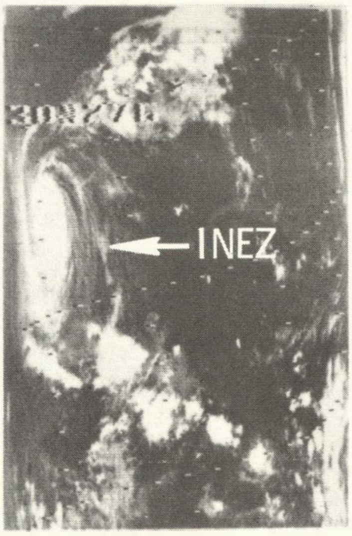

30°N
20°N
10°N

100°W 90°W

INEZ 1966
NIMBUS II HRIR
OCT. 10, 1966

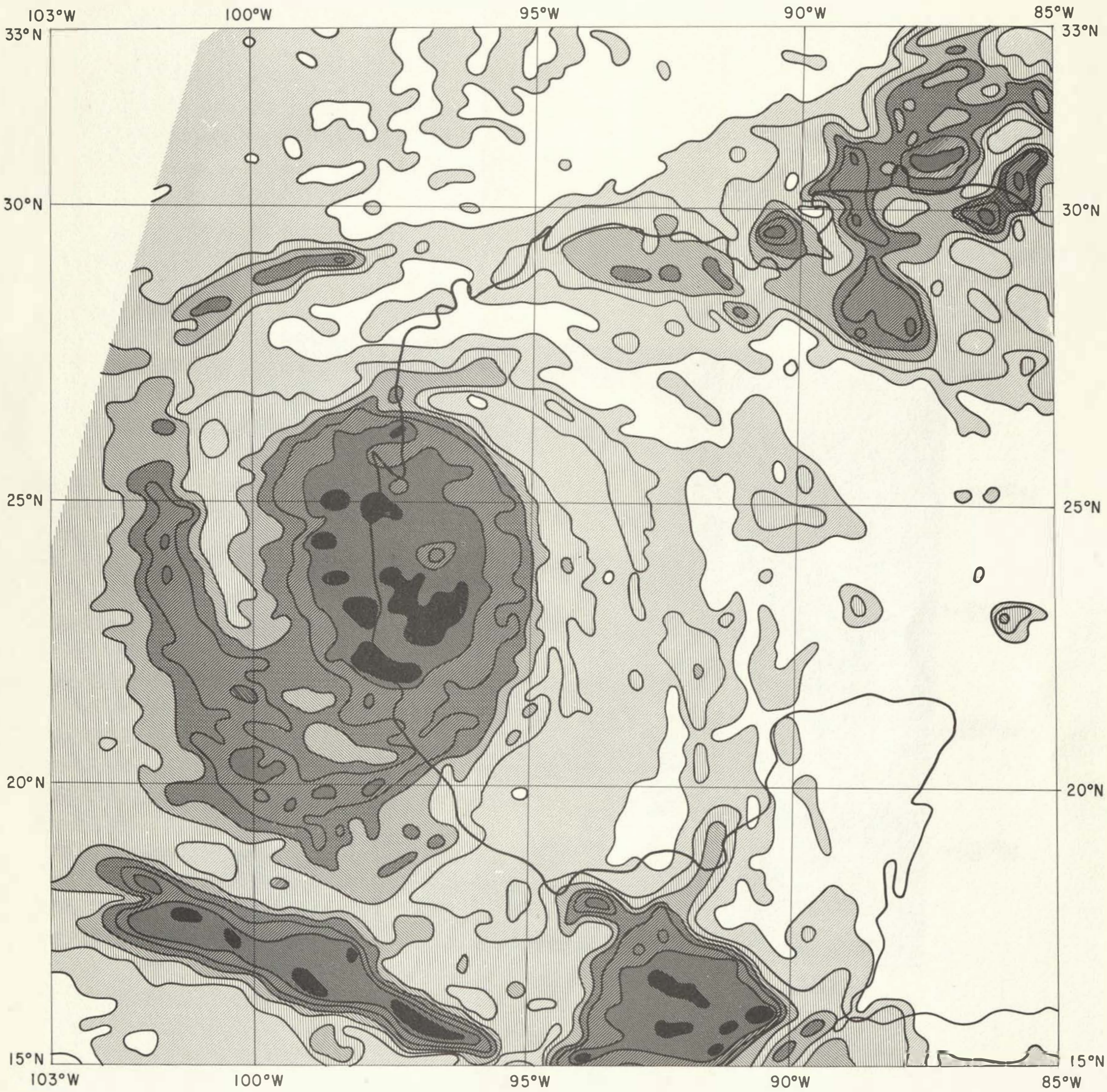

EQUIVALENT BLACKBODY TEMPERATURE (°K)

< 230° : > 11 km	270° — 280° : 3.5 — 5.0 km
230° — 240° : 9.5 — 11 km	280° — 290° : 1.5 — 3.5 km
240° — 250° : 8.0 — 9.5 km	> 290° : 0 — 1.5 km
250° — 260° : 6.5 — 8.0 km	
260° — 270° : 5.0 — 6.5 km	

HURRICANE INEZ, 1966

NIMBUS II HRIR

OCTOBER 10, 1966

Figure A-60

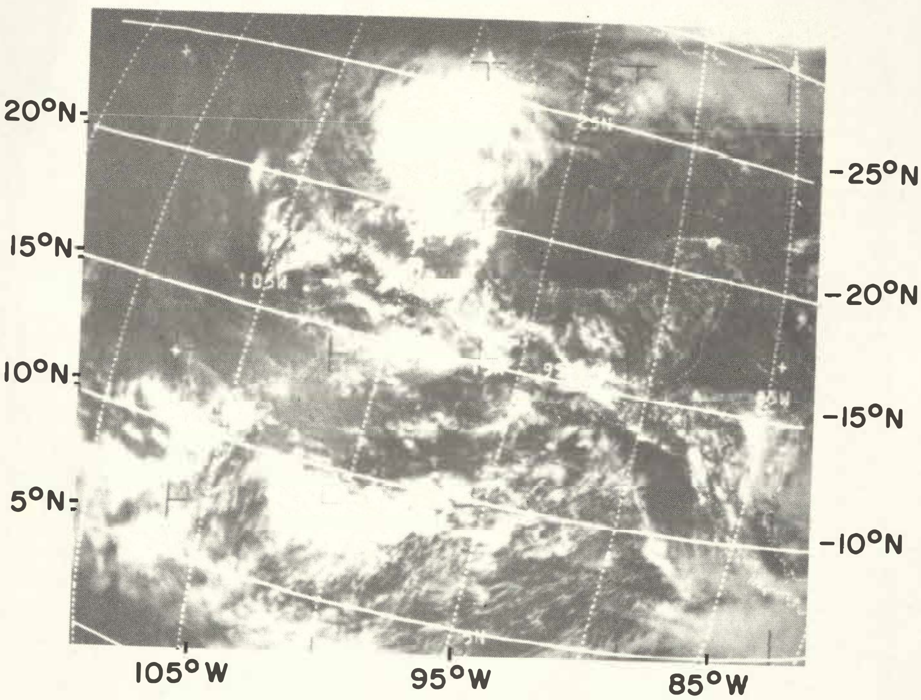

INEZ 1966
ESSA III TV
OCT. 10, 1966